FFI-rapport 2015/00402

NATO Narrowband Waveform (NBWF) – performance analysis of complex networks

Tore J. Berg

FFI Forsvarets forskningsinstitutt

NATO Narrowband Waveform (NBWF) – performance analysis of complex networks

Tore J. Berg

Norwegian Defence Research Establishment (FFI)

9 April 2015

FFI-rapport 2015/00402

1295

P: ISBN 978-82-464-2514-6
E: ISBN 978-82-464-2515-3

Keywords

Modellering og simulering

Datamaskinnett

Radiosamband

Trådløs kommunikasjon

Approved by

Jan Erik Voldhaug	Project Manager
Anders Eggen	Director

English summary

NATO is in the process of finishing edition 1 of the narrowband waveform (NBWF) STANAGs 5630 to 5633. NBWF provides ground-to-ground communication between troops/platforms at the tactical battlefield using the military VHF and UHF band (30 – 500 MHz). NBWF is a single-channel mobile ad-hoc radio network (MANET) which shall serve voice and data traffic using radio frequency (RF) bandwidth less than 100 kHz, primarily 25 kHz.

FFI has participated in the NBWF standardisation activity for a number of years, and many simulation experiments have been executed to analyse different technical solutions. In our earlier simulation experiments, we analysed simple NBWF networks with few radio nodes. Now we extend the network size (number of nodes) and use scenarios with more demanding radio conditions. The experimental results obtained through simulations did not discover any anomalous behaviour of the NBWF protocols. As a network increases in size, the routing traffic increases also. The simulator used did not model the NBWF routing protocols, but used static routing. We expect that the routing protocol is the protocol that would be the major obstacle to deploy large networks.

As an NBWF network turns from a fully meshed topology with single-hop traffic to a multi-hop scenario with hidden nodes, the NBWF protocol efficiency decreases. By gradually decreasing the radio range, we illustrated how the network throughput decreases with reduced radio coverage. Multi-hop IP-streams consume more transmission capacity than single-hop IP-streams and therefore, the network throughput must decrease. The simulation experiments showed that it is the medium access reservation protocol that gets the toughest operating conditions in the scenarios analysed due to the hidden node problem.

Sammendrag

Nato har en pågående aktivitet der det skal utvikles en smalbånds radiobølgeform (NBWF) standard (STANAG). NBWF er et ad-hoc nettverk der nodene kommuniserer over en en-kanals radiokanal med RF-båndbredde mindre enn 100kHz.

FFI har deltatt i NBWF-standardiseringsarbeidet i mange år. Forskjellige tekniske løsninger har blitt analysert basert på data fra simuleringseksperimenter. Tidligere analyser har bare vært utført på enkle nettopologier. Denne rapporten utvider kompleksiteten både ved å øke antall noder og ved å innføre redusert radiodekning.

Virkningsgraden til NBWF-protokollene må nødvendigvis gå ned etter hvert som radiodekningen reduseres og nettet får flerhoppsruter og skjulte noder. NBWF-protokollene viser ingen unormal oppførsel og gir en gradvis reduksjon i ytelsen etter hvert som radiodekningen blir dårligere.

Contents

1 Introduction

NATO is in the process of finishing edition 1 of the narrowband waveform (NBWF) STANAGs [6, 7, 8, 9]. NBWF provides ground-to-ground communication between troops/platforms at the tactical battlefield using the military VHF and UHF band (30 – 500 MHz). NBWF is a single-channel mobile ad-hoc radio network (MANET) which shall serve voice and data traffic using RF bandwidth less than 100 kHz, primarily 25 kHz. NBWF employs time division multiple access (TDMA) and a dynamic reservation protocol to allocate transmission capacity for voice and data. This reservation protocol is based on a random access protocol [8, chapter 5].

FFI has participated in the NBWF standardisation activity for a number of years. Many simulation experiments have been conducted to analyse different technical solutions [1, 2, 3]. In our earlier simulation experiments, we analysed simple NBWF networks with few radio nodes. Now we extend the network size and even evaluate larger networks than the NBWF standard is intended to handle.

This document is written for readers with detailed knowledge of the NBWF STANAG proposals [6, 7, 8, 9].

This document is organised as follows. Chapter 2 “Adaptive MAC – a revised construction” corrects a mistake in [1] and modifies the adaptive Medium Access Control (MAC) function. Chapter 3 “MAC Parameter Optimization” uses simulation experiments to find the best MAC parameters for an NBWF network with 25 radios. It is interesting to know how robust the NBWF protocols are when the network size becomes larger than the intended size. A fully connected mesh topology is used in chapter 4 “GridN*n* at 50W” to analyse networks with 16, 36 and 100 nodes. Note that the NBWF simulator does not model routing and hence, no routing traffic will flow in the network. The load of routing traffic is expected to take much capacity in large networks. It is anticipated that the routing protocol will limit the number of nodes more than the MAC protocol.

As the radio coverage decreases, it is the MAC protocol that gets the most inconvenient operating condition first. At some point the MAC protocol will fail to control the access to the radio channel, and the network enters a chaotic state. Two phases are foreseen:

Phase 1: The MAC CR PDU[1] suffers from the hidden–node problem [2, chapter 2] and it becomes difficult to establish MAC connections.
Phase 2: Nodes fail to track the MAC reservations and start to send when other nodes have succeeded to establish connections. This leads to packet loss during the data transfer phase and the LLC[2] entity starts to retransmit.

[1] MAC Connect Request Protocol Data Unit
[2] Logical Link Control

Chapter 5 “GridN100 Networks” analyses a scenario where the radio coverage switches from excellent to bad.

Any network must constrain how long a packet can reside in the network. At FFI we originally implemented a packet lifetime control in the NBWF simulator based on a network based lifetime control scheme: the entry-node adds a remaining lifetime field of 60 seconds to every IP-packet and the network nodes decrement this value as the packet is forwarded to the sink-node. When the remaining lifetime field becomes zero, the packet is deleted silently. Later FFI proposed to use a node based lifetime control scheme [9]. Chapter 6 “Packet Lifetime Control” looks at the differences between these two methods.

All the layers in the NBWF protocol support Multi-Level Precedence and Pre-emption (MLPP). Reference [1] has analysed the MLPP performance in fully meshed topologies. As the network topology becomes fragmented, it becomes more demanding to maintain good priority sorting characteristics. Chapter 7 “Priority Handling in Multihop Networks” considers this case.

1.1 Terminology

The first part of this section defines the most important terms used in this report, while the second part specifies the probes used and describes what they measure. An NBWF network is a stochastic process and a probe is the tool for observing the network behaviour. In the simulator, a probe is a software component/object which collects data (e.g., end-to-end packet delays) and produces an estimate of the first order moment.

Busy/active/idle node
A busy (or active) node has outgoing traffic while an idle node has not.

AHAnN
All-hearing-all (AHA) refers to a network topology where all the nodes have overlapping radio coverage areas (fully connected topology). n*N* specifies an AHA-network containing *N*-nodes (e.g. AHAn25).

The near-far problem
A receiver is locked to a weak signal from a distant node when a node in the vicinity starts to emit a high energy signal. The stronger signal overrides the weaker signal and the first packet is lost.

Sink-node
An end-destination for an IP traffic stream.

Entry-node
A radio node which is the end-source node for an IP traffic stream (fresh input traffic) from an IP client.

Edge-node
A node taking the role as *sink-node* and/or *entry-node*.

Throughput capacity
When the IP traffic requests use of automatic repeat request (ARQ), the offered traffic and the throughput shall follow a straight line up to the point where the radio channel becomes congested, see Figure 1.1. The throughput capacity is defined as the point on the curve where the deviation between the offered traffic and the throughput becomes higher than approximately 1%.

Maximum throughput
The highest point on a throughput plot, see Figure 1.1. Only loss tolerant IP applications can operate at this load level.

Below we specify the probes used in this report.

P(receive CC), p_{CC}
This estimator is implemented in the MAC layer. When MAC has sent a CR PDU[3], it expects to receive a CC PDU. If a CC[4] PDU is received, the value sampled is one. Otherwise, zero. Two or more CR PDUs may be sent simultaneously (i.e., a packet collision event), but then the probability that one of the MAC entities gets a CC PDU is low since NBWF demands a positive signal-to-noise ratio (SNR) to generate a carrier-sense (CAS), reference [15, table B.2]. p_{CC} samples are also collected for LLC SDUs[5] that reach the age limit

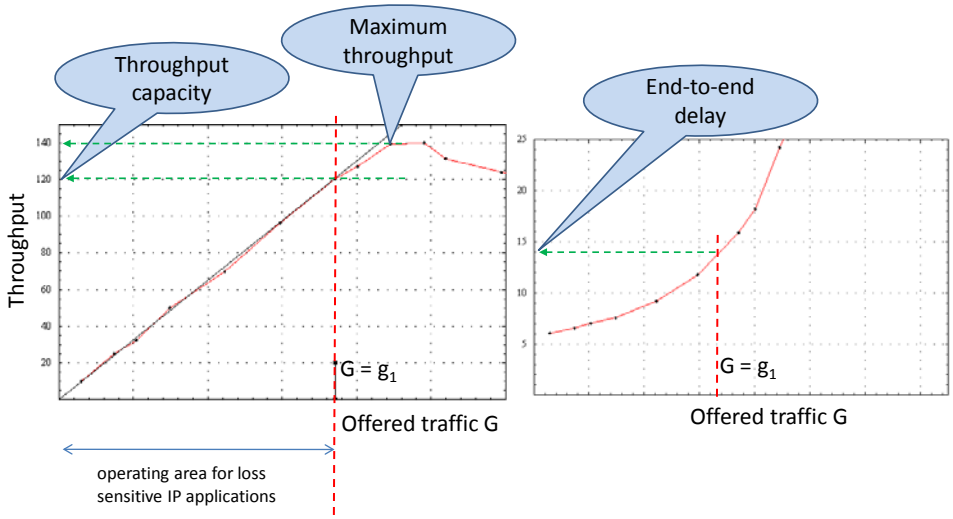

Figure 1.1 Throughput and delay plot examples.

[3] Connect Request Protocol Data Unit
[4] Connect Confirm
[5] Logical Link Control Service Data Unit

Throughput [bytes/s], λ

All the network layer entities in the sink-nodes report the payload size to this probe when they receive a packet destined for the IP client. This probe measures the average number of bytes received over a time window of 1 second and sends this value to a batch-means module [11].

End-to-end delay [sec]

In the simulator, all packets get a timestamp when they are created and the sink-nodes are then able to calculate their age. Of course, lost packets due to buffer overflow, or lifetime expiry, are not included.

MAC load level

As described in reference [1, chapter 3], every NBWF node takes traffic load level measurements continuously. This load state is sampled as either high (sample value 1) or low (sample value 0). Samples are collected at the time instances where the MAC entity draws its random access delay.

MAC busy CR nodes, N_{busy} (N_{Gbusy})

With "busy CR nodes" we mean the number of nodes that have outgoing CR PDU(s). The MAC scheduling process operates on CR PDUs, and not DT PDUs. Each node tracks the number of busy nodes in their neighbourhood by using the process described in [1, chapter 3].
The simulator has implemented an additional version of this probe *(N_{Gbusy})* giving improved accuracy. This probe does not rely on signalling across the radio channel but is implemented by using a global object in the simulator. Both probes are important since the adaptive MAC scheduling process is based on samples from the N_{busy}-distribution. However, the N_{Gbusy}-probe can only be implemented in a virtual world and its benefit is a more correct view of the network state. For example, lost messages do not affect its accuracy.
N_{Gbusy} - and N_{busy}-samples are collected at the time instances where the MAC entity draws a random access delay.

Number of connection request recoveries, N_{CRR}

This estimator is implemented in the LLC layer. If the MAC entity has sent a CR PDU and no CC PDU is received within a certain time limit, the MAC entity shall issue a MAC-Disconnect.indication with the reason parameter "missing CC". Upon this event, the LLC entity initiates the LLC exponential backoff process described in [8, section 4.2.5.5]. The LLC entity shall, after a short time period, recover from the setup failure by repeating the connection setup process. The LLC entity continues until a MAC connection is established, or the LLC SDU lifetime expires. The N_{CRR}–probe measures the number of setup attempts per LLC SDU. N_{CRR}=0 means that LLC always succeeds in the first attempt; no recovery required. An N_{CRR}–sample is collected upon successful connection setup and upon LLC SDU lifetime expiry. When the LLC entity has issued a MAC-Connect.request, MAC shall respond with one of the responses:
r1: *MAC-Connect.conf* => successful setup
r2: *MAC-Connect.ind* => another node reserved the channel
r3: *MAC-Disconnect.ind* (reason MissingCC) => setup failure

If r1 occurs, the sample value one is saved. If r3 occurs, the sample values zero is saved. No sampling is done if r2 occurs.

LLC ReTx ratio, N_{retx}

This estimator is implemented in the LLC layer and sample *i* is formed as:

s_i = 1+"number of bytes retransmitted"/"LLC SDU byte size".

The sample is taken when the LLC entity issues a *MAC-Disconnect.request*. LLC SDUs deleted by the lifetime control function are not included in the statistics. $N_{retx} = 1$ means no retransmissions.

LLC Setup delay [sec]

The latency time measured between the **first** *MAC-Connect.request* and the corresponding *MAC-Connect.confirm* which results in a *MAC-Connect.confirm*. Generally, the LLC entity must issue a number of requests before it wins the channel, see Figure 1.2.

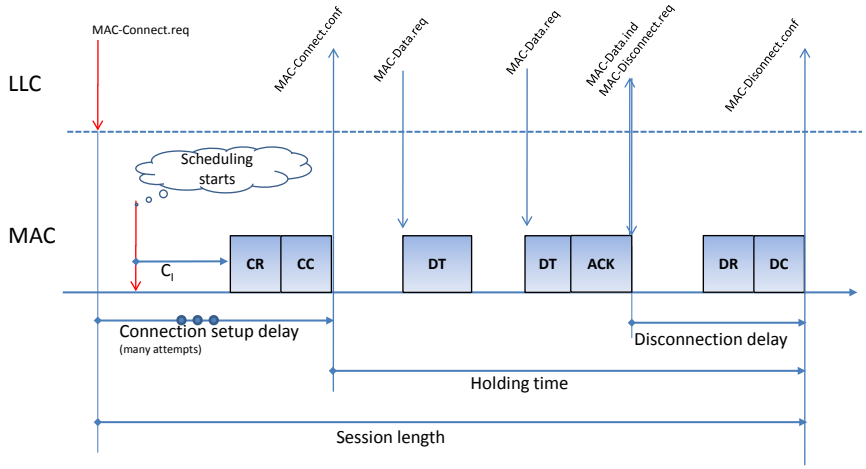

Figure 1.2 MAC delivery cycle when ARQ is enabled. A node must generally take part in a number of access cycles before it wins the channel access.

2 Adaptive MAC – a revised construction

The purpose of this chapter is to correct an error in reference [1, section 6.3]. This reference writes about a design flaw in the MLPP adaptive MAC algorithm and states:

s_1) "A design flaw in the load state switching strategy in chapter 5 is that all the priority levels are handled separately."
s_2) "Then the network with asymmetric priority distribution did never enter the high-load state and may suffer from a high collision rate."

Sentence s_2 is incorrect. The maximum number of busy nodes per priority level is {7,6,6.6} [1, page 35]. Hence, the threshold values [1, TS4 set on page 20] can never be reached. Priority levels with overlapping random delay ranges should be considered as a group. A solution to s_1 is expressed by the following program section:

```
updateStateDiagrams()
{
    //Step 1: read the estimated number of busy nodes and update the diagrams
    1.  for( all i in {{P3},{P2},{P1},{P0},{P3,P2},{P2,P1},{P1,P0},{P2,P1,P0}} )
    2.    int n = getNumberOfBusyNodes( i );
    3.    newMLLreport( i, n );
    4.  endfor;
    //Step 2: Test the single priority levels in the order P3...P0
    5.  if( isHighLoad({P3}) )
    6.    //Set high load on P2...P0 to maintain the sorting characteristics
    7.    forceHighLoad( {{P2},{P1},{P0}} )
    8.  elseif( isHighLoad({P2}) )
    9.    forceHighLoad( {{P1},{P0}} )
    10. elseif( isHighLoad({P1}) )
    11.   forceHighLoad({{P0})
    12. endif
    //Step 3: Test the combined priority levels. Start at highest level!
    13. if( isHighLoad({P3,P2}) )
    14.   forceHighLoad( {{P3},{P2},{P1},{P0}} )
    15. elseif( isHighLoad({P2,P1,P0} or isHighLoad({P2,P1}) )
    16.   forceHighLoad( {{P2},{P1},{P0}} )
    17. elseif( isHighLoad({P1,P0}) )
    18.   forceHighLoad( {{P1},{P0} )
    19. endif
} // end updateStateDiagrams
```

The lines 13 to 19 add the new functionality required to test combined priority levels. Line 1 expresses that a radio node shall implement eight finite state machines (FSM), see Figure 2.1, instances instead of four. Recall that [1, chapter 3]:

$$Ema(N(t)) = \quad n_{i+1} = (1-\gamma)\cdot n_i + \gamma \cdot N(t_{i+1}), \quad n_0 = 0, \qquad 0 < \gamma < 1$$

Line 2 reads the accumulated MLL-reports. If $N_{P3}(t)=1$ and $N_{P2}(t)=5$ then a correct implementation fulfil:

getNumberOfBusyNodes({P3})==1 and *getNumberOfBusyNodes({P3,P2})==6*.

Line 3 sends the samples to the corresponding FSM, and the function *newMLLreport()* must execute *Ema(N(t)), Inst(N(t))* and must set *isForcedHighLoad=false*, while *forceHighLoad()* must do the opposite; *isForcedHighLoad=true*. *isHighLoad()* shall act as follows:

```
bool
isHighLoad( FSMindex i ) {
    1.  if( fsm[i].isForcedHighLoad ) return true; // This test first!
    2.  return fsm[i].state == FsmHighLoad; // State diagram in figure 2.1
} // end isHighLoad()
```

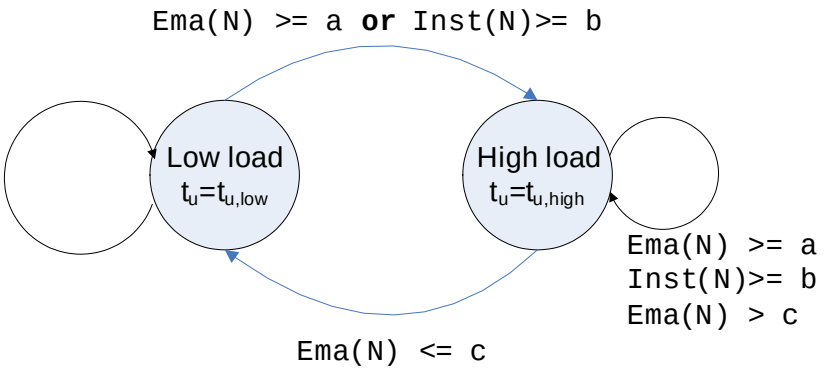

bool isForcedHighLoad

Figure 2.1 *Finite State Machine (FSM) for tracing the MAC load level. An NBWF node must implement one FSM for each of the eight priority groups, see updateStateDiagrams() line 1. isForcedHighLoad is an additional FSM variable. The following rule must be fulfilled: c < a < b.*

A network handles 1/0.2025=4.9 MLL-reports per second since the reports are sent in a TDMA super frame slot. To save processing resources in the radio nodes, the FSMs can be updated at a much slower rate. However, the *N(t)*-function [1, figure 3.2] must be updated at the MLL-report rate. In a 25-node network, the MLL-report period per node is 5 seconds and to update the FSMs faster than this is futile. Let T_{fsm} denote the FSM update period. To have smoother MAC scheduling shifts in the network, we make the T_{fsm} stochastic:

$$T_{fsm} = t_{fsm} \bullet RandomUniform[0.5,1] \quad (2.1)$$

Now, the speed of the *Ema(N(t))* and the *Inst(N(t))* updates depend on the two parameters t_{fsm} and γ. We use a fast update rate t_{fsm} =10 seconds (=>T_{fsm} range 5...10) and set the γ=0.1; small γ-values smooth out the samples more than large values. The nodes are still able to react fast to a transient due to the *Inst(N(t))*–function.

3 MAC Parameter Optimization

This chapter goes through the MAC parameter optimization process for an AHAn25-network that shall serve the traffic specified in Table 3.1. There are far too many steps to be presented in this report. Only the most important results are included. All the adaptive MAC modifications outlined in chapter 2 are now implemented in the simulator.

Parameter name	**Value**
Packet arrival distribution	Poisson
Packet length (layer 7)	Fixed 500 bytes
Priority distribution {P0(lowest),...,P3}	{0.1,0.4,0.4,0.1}
Traffic pattern	unicast “all-to-all”
Maximum packet lifetime	60 seconds
Link ARQ	enabled

Table 3.1 Traffic generator parameters.

While reading this chapter, keep in mind that we cannot find a MAC parameter set to be claimed as a winner for all scenarios. In fact, this also applies to a fully connected network operating in a perfect radio environment. MAC parameter optimization is a process that must do many trade-offs.

AHAn*N* refers to a grid network where all the *N*-nodes have overlapping radio coverage areas. Routing and relaying are not required since all the destinations are reached in one radio hop. With “excellent radio environment”, we mean a network with insignificant background noise and with optimum received signal level; a high level without overloading the receiver input.

The purpose of this chapter is to analyse a fully connected network serving MLPP traffic under excellent radio conditions. In later chapters, we gradually reduce the transmitting power to get scenarios with more challenging radio conditions. This chapter will then serve as a reference.

Our earlier experiments [1, 2, 3] have mostly used a fixed pathloss model and then all the transmissions have equal power at the receivers. To have scenarios closer to real-world scenarios, this report uses an Egli pathloss model [4,5]. Assuming a vehicle mounted radio, we use the radio parameter values specified in Table 3.2. The NBWF radio airframe constitutes the four different sections [7, figure 2-3]: Preamble (E+P), Start-Of-Message (SOM), Parameter Register (PAR) and the payload. We configure the networks to use the N1-interleaver (20kbps) for payload transmissions. Table 3.3 presents the dynamic detection ranges for the different air frame sections. The term “dynamic” refers to the fact that the detection probability is given by a stochastic model within the radio ranges shown. For a shorter distance, the detection is always successful in presence of Gaussian noise only (i.e., no packet collisions). Detection is impossible over longer distances.

Parameter name	Value
Terrain model	Egli
Antenna height	3 meters
Antenna gain Cable loss	0 dB
Transmitter power	50 W
RF frequency	50 MHz

Table 3.2 Radio parameters.

PHY field	Dynamic detection range
Preamble	$31 \leq r \leq 47$ km
SOM	$39 \leq r \leq 47$ km
PAR	$38 \leq r \leq 54$ km
N1 (20kbps payload)	$31 \leq r \leq 37$ km

Table 3.3 Radio range for the radio data in Table 3.2.

A radio node must receive the preamble-field and the SOM-field to detect a busy radio channel. If a node switches from send state to preamble-search state within an on-going (preamble+SOM)-period, this node is unable to detect the transmission and acts as if the channel is idle. A successful packet reception is conditioned on four sequential events: e_1) Preamble detection e_2) SOM-detection e_3) PAR-detection and e_4) Error-free payload. A packet loss event occurs if any of these four events fail. As shown in the Table 3.3, the sections of the air frame have different radio ranges and generally, the nodes behave differently on the playground. However, the playground in Figure 3.1 has a fairly homogenous group of nodes since all the radio links are shorter than 31 km.

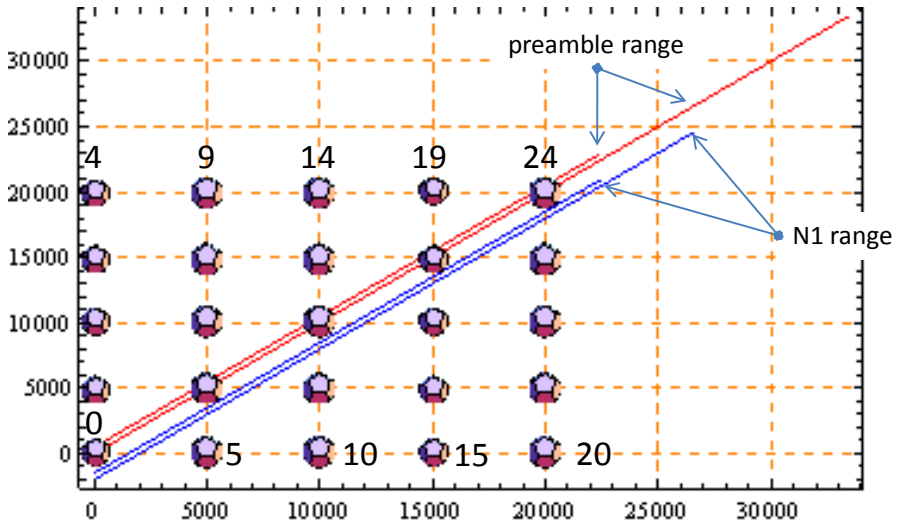

Figure 3.1 The GridN25 network deployed in an operating area of 20x20 km^2. The figure is marked with the preamble and the N1-interleaver dynamic ranges.

Each node on the playground has its own traffic generator. All traffic generators are identically configured with the parameter values presented in Table 3.1. Due to the fact that it is the MAC CR PDU that is hit by collisions, and not the IP packet itself, the NBWF protocol *efficiency* is less sensitive to the IP packet length[6]. Therefore we do not need to use the packet length as a simulation parameter and use 500 bytes fixed sized payload. When a network gets into trouble, a link ARQ protocol often fortifies the problem. This means that it is easier to discover problems and use of link ARQ is the default to use here.

3.1 Symmetric Traffic

We continue to use the MAC parameters from [1, chapter 5], but change the priority delays slightly. Table 3.4 summarises the values to be used in the first simulation experiment.

Set number	FSM load state	Priority	Priority delay	Random delay t_u
1	Low	P3	0 msec	25 msec
		P2	10	50
		P1	20	75
		P0	30	100
	High	P3	0	100
		P2	10	200
		P1	20	300
		P0	30	400

Table 3.4 MAC random access parameters in msec. Set 1.

The simulator radio parameter settings are rx-to-tx-turn-time 1 msec and preamble length 1.5 msec, giving a 2.5 msec latency for detecting a transmission at the receivers. The probability of collision can be expressed as $p_{coll} = 1 - (1 - 2.5/t_u)^n$ [1, equation 5.2], where t_u is the numbers in the rightmost column in the table above. To obtain a starting point for selecting *{a,b,c}*-values in Figure 2.1, Figure 3.2 plots the theoretical probability of collision versus the number of busy nodes.

First consider the upper plot, which applies for scheduling under low load. The dimensioning rule selected is to keep the collision rate less than 20%. Hence, the plot tells that $\{a_{P0},a_{P1},a_{P2},a_{P3}\} = \{9,7,4,2\}$ should be used, but we do not want P3 to shift to high-load scheduling too early and use $\{a_{P0},a_{P1},a_{P2},a_{P3}\} = \{9,7,4,3\}$. Similarly, we use the collision rate switching threshold 40% for the *b*-parameter, giving $\{b_{P0},b_{P1},b_{P2},b_{P3}\} = \{20,15,10,5\}$. The $(1\text{-}p_{CC})$-distribution is different from the p_{coll}-distribution but, of course, a low collision rate improves the MAC CR PDU success rate.

[6] Of course, the throughput/delay performance is strongly affected.

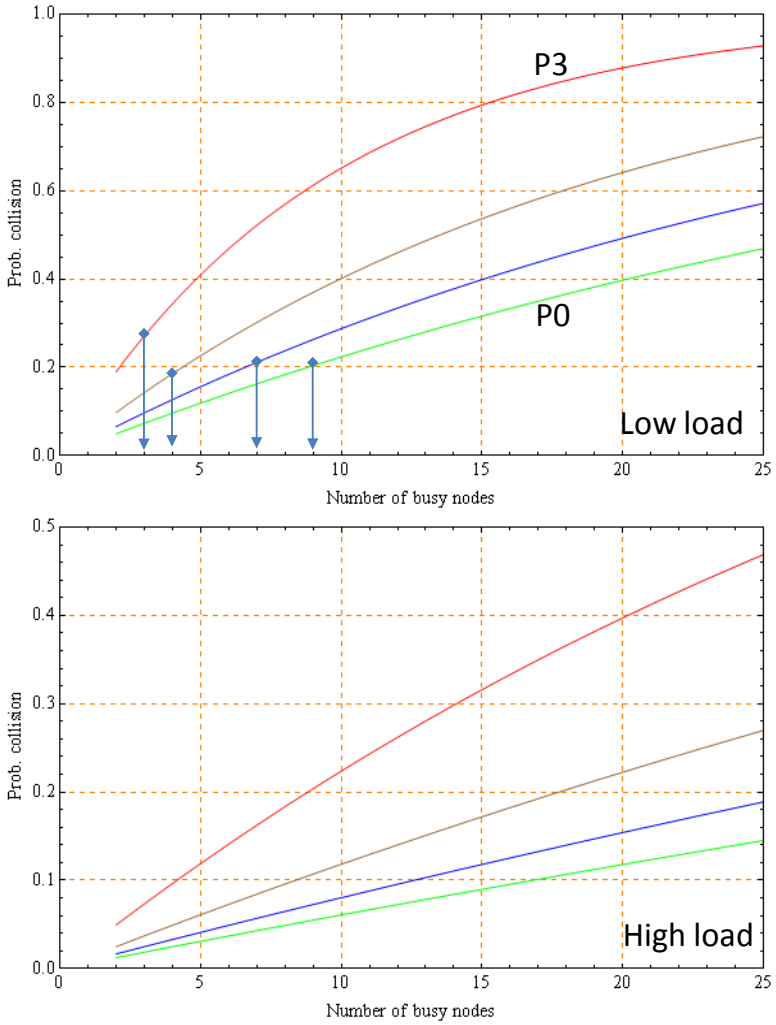

Figure 3.2 Theoretical probability of collision versus number of busy nodes. The vertical arrows mark the up regulation threshold values.

The next question to answer is how the *c*-parameter shall be set. To prevent a fast switching between the low- and the high-load states, we should apply a hysteresis coefficient, given by the difference *a*-*c*. Table 3.5 shows the *c*-values selected.

Set number	FSM instance	a	b	c	γ
1	{P0}	9	20	4	0.1
	{P1}	7	15	4	
	{P2}	4	10	3	
	{P3}	3	5	2	
	{P3,P2}	4	10	3	
	{P2,P1}	7	15	4	
	{P1,P0}	9	20	4	
	{P2,P1,P0}	9	20	4	

Table 3.5 FSM parameters. Set 1.

Now it is time to run a simulation experiment to see how the AHAn25 performs with the new MAC parameters. As illustrated by Figure 3.3, the overall network throughput has a satisfactory course compared to our design goals [1, chapter 2]. However, to give the P2-throughput a more linear progress, the MLPP function should have dropped more P1-packets around Λ = 1000 bytes/s. This can be achieved by increasing the P1-priority delay. Another objection to parameter set 1, is the switching point from low-load state to high-load state, see Figure 3.4.

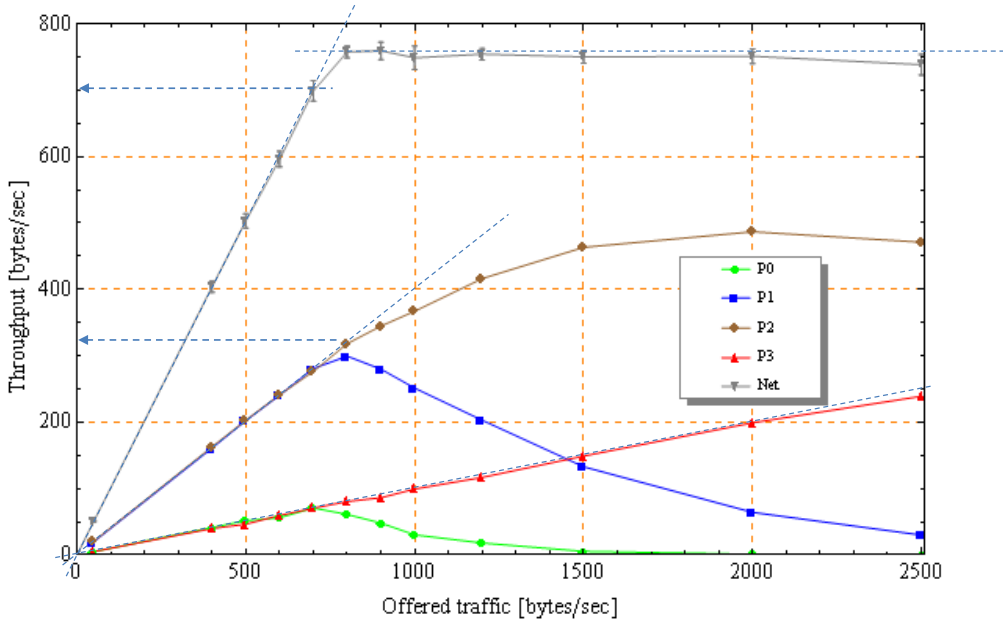

Figure 3.3 AHAn25 throughput as 90% confidence intervals when using MAC parameter set 1 (simAug26a).

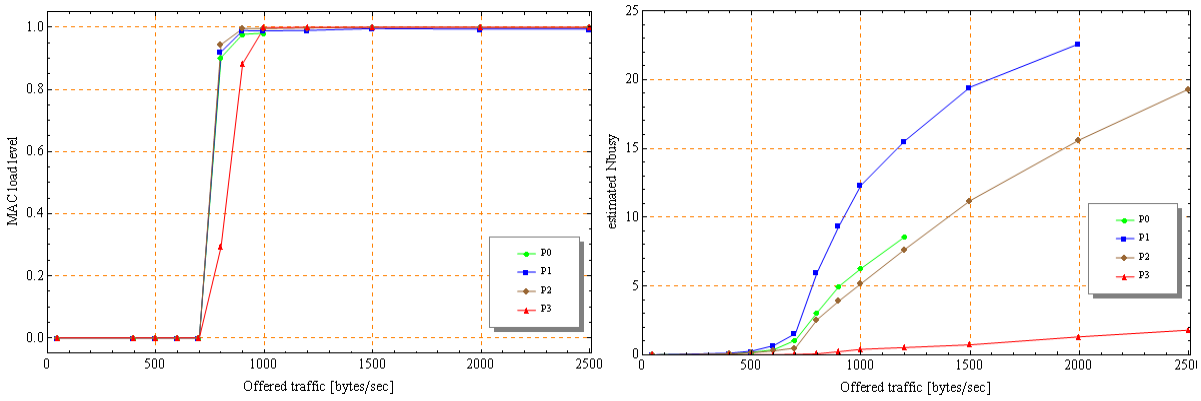

Figure 3.4 Simulated MAC load level(left) and N_{busy} for MAC parameter set 1 (simAug26a).

$N_{P3,busy}$ is near zero (rightmost plot in Figure 3.4) and the switching should be done at a higher load. This switching must be trigged by FSM_{P3P2}. Therefore simulation experiment number 2 use FSM_{P3P2}(a,b,c)=(12,20,7) where the *a*-value (=1+11) is taken from N_{busy}-plot at Λ = 1500 bytes/s. With this modification, the P3 MAC load level turned to high-load at a higher traffic load as wanted. Also the P2 and P1 levels should switch to high-load state later, so we applied the same

cure on the other combined priority levels *{{P2,P1},...,{P2,P1,P0}}*, and then executed experiment number 3. Figure 3.5 illustrates how the MAC load level regulation improved.

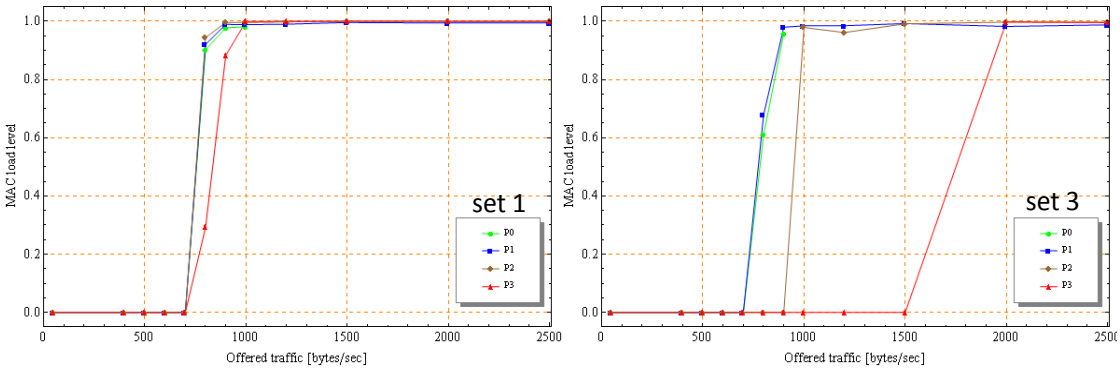

Figure 3.5 MAC load level comparison for the simulation experiments 1 and 4.

Simulation experiment 4 and 5 focused on adjusting the "priority leaks" in Figure 3.3 by increasing the priority delays. Figure 3.6 illustrates the throughput plot from experiment 4. Compared to Figure 3.3, we clearly see the drawback of reducing the (P0+P1)-priority leaks. The network throughput shape deviates more from the design goal and the network throughput capacity drops from 700 to 650 bytes/s. On the positive side, the P2-throughput increases from 320 to 400 bytes/s, and the {P3,P2}-LLC setup delay in Figure 3.7 decreases significantly at Λ=1500 bytes/s. Experiment 5 produced even more P2-throughput, but the network throughput capacity loss was too high (700 vs. 550 bytes/s). Note the excellent linearity of the P3-throughput curves in all the experiments. We select the parameters used in experiment 4 as the final set, see Table 3.6 and Table 3.7.

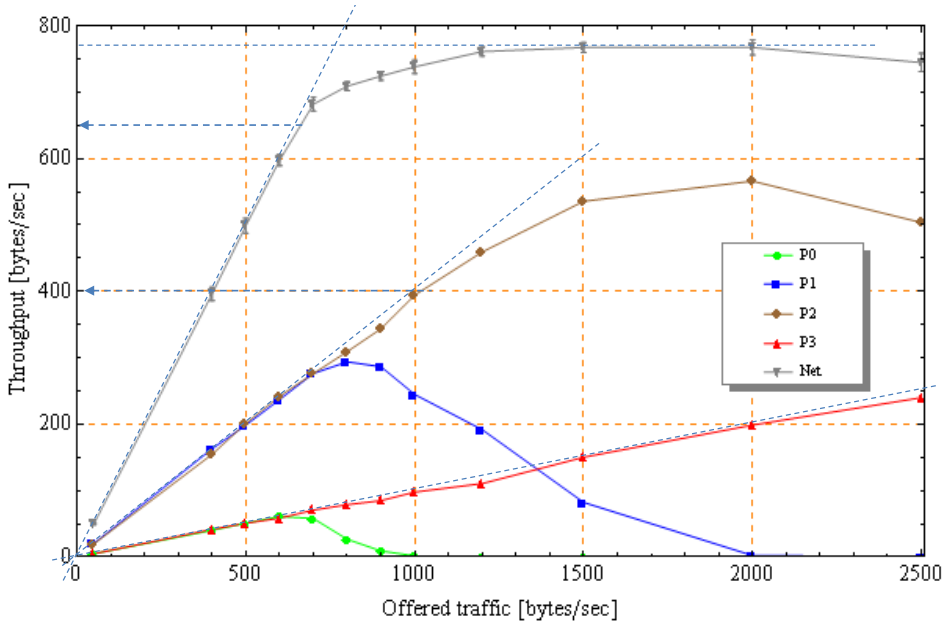

Figure 3.6 AHAn25 throughput as 90% confidence intervals when using MAC parameter set 4 (simAug26a).

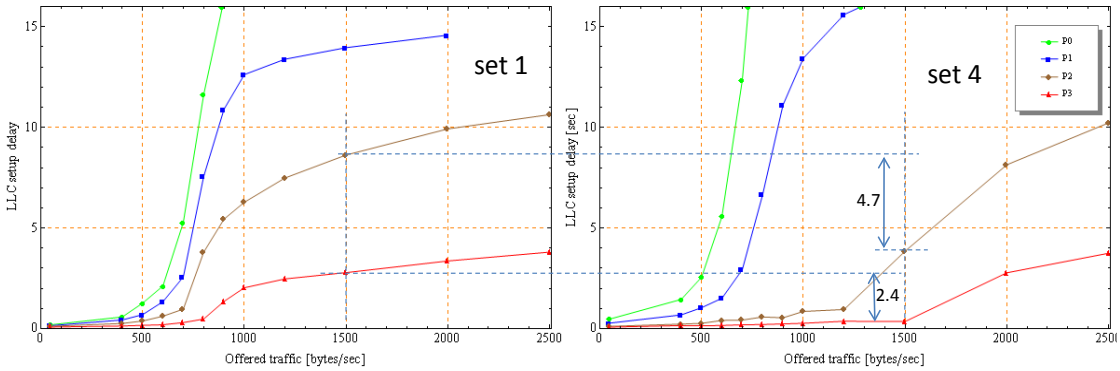

Figure 3.7 LLC setup delay comparison for the simulation experiments 1 and 4.

Set number	FSM load state	Priority	Priority delay	Random delay t_u
4	Low	P3	0 msec	25 msec
		P2	10	50
		P1	80	75
		P0	180	100
	High	P3	0	100
		P2	10	200
		P1	80	300
		P0	180	400

Table 3.6 MAC random access parameters in msec. Set 4.

Set number	FSM instance	a	b	c	γ
4	{P0}	9	20	4	0.1
	{P1}	7	15	4	
	{P2}	4	10	3	
	{P3}	3	5	2	
	{P3,P2}	15	25	8	
	{P2,P1}	25	30	12	
	{P1,P0}	15	25	8	
	{P2,P1,P0}	55	5000	25	

Table 3.7 FSM parameters. Set 4. The last line sets b=5000 and this disables the InstN(t) test for that FSM.

3.2 Symmetric vs. Asymmetric Traffic

In the scenario simulated above, the nodes had homogeneous traffic conditions and the nodes switched to the next higher priority level at the same load level. Now we specify a new scenario, using the same relative offered traffic per priority, but with an inhomogeneous priority distribution over the nodes:

Node address set P0[7]	{0,...,6}	P0-traffic:	$\Lambda_{P0} = 0.1 \cdot \Lambda$
...P1	{7,...,12}	P1-traffic:	$\Lambda_{P1} = 0.4 \cdot \Lambda$
...P2	{13,...,18}	P2-traffic:	$\Lambda_{P2} = 0.4 \cdot \Lambda$
...P3	{19,...,24}	P3-traffic:	$\Lambda_{P3} = 0.1 \cdot \Lambda$

Regardless of the traffic level, here the nodes in the set {0,...,6} serve P0-traffic only. The P0-group contains 7 elements while the others have 6 elements. In the previous scenario, we observed up to 23 nodes which scheduled P1-traffic (Figure 3.4). Now this number cannot become larger than 6.

Throughput versus offered traffic for the asymmetric traffic case using MAC parameter set 4 is shown in Figure 3.8. The first impression is that the MLPP MAC service handles the traffic as it should. From the simulation output, we read the following throughput capacities and link delays (Figure 3.8):

Traffic/priority	P0	P1	P2	network
Symmetric	60 bytes/s at 6 sec	280 bytes/s at 5 sec	400 bytes/s at 13 sec	600 bytes/s at 2.3±0.2
Asymmetric	50 bytes/s at 4 sec	280 bytes/s at 5sec	400 bytes/s at 2 sec	600 bytes/s at 2.5±0.3

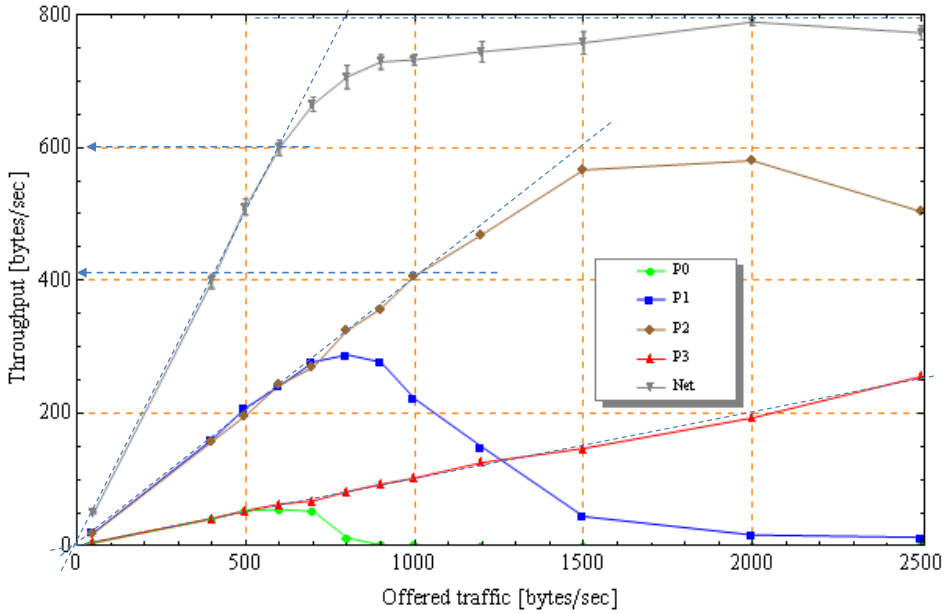

Figure 3.8 AHAn25 throughput as 90% confidence intervals under asymmetric traffic (simAug27a).

For the P2 and P3 link delay performance, we observe a significant difference. Compared to the asymmetric network, the N_{Gbusy}-plot in Figure 3.13 indicates that the symmetric network has more (P0+P1)-busy nodes in the range $\Lambda \in [700,1500]$. This implies that an arriving P2- or P3-packet

[7] We have 25 nodes and 4 priority levels. The P0-group contains 7 elements, the other 6.

must wait for service until the lower priority packet has been served[8]. Therefore, under symmetric traffic conditions, the P3 link delay is "pushed upwards" by the other priorities, while the asymmetric traffic case provides a flat P3 link delay which conforms to our design goal as explained in reference [1, chapter 2].

Also note the similarity between the N_{busy}–plot (Figure 3.12) and the N_{Gbusy}–plot (Figure 3.13) for the asymmetric network. An MLL-report does not signal load level per priority, but since each node serves one priority only, the MLL-report is able to signal the exact queue status.

The most direct view of the MLPP service is given by the LLC connection setup delay since this stochastic variable tells us how fast a high priority packet is able to grab the radio channel compared to the lower priority packets. The durations of the data transfer phase and the disconnection phase are not affected by the priority level. As seen from Figure 3.10, the low priority packets get a much longer delay with increasing load. Fewer nodes have P3 traffic in the asymmetric traffic case and P3 high-load MAC scheduling is never entered (Figure 3.11).

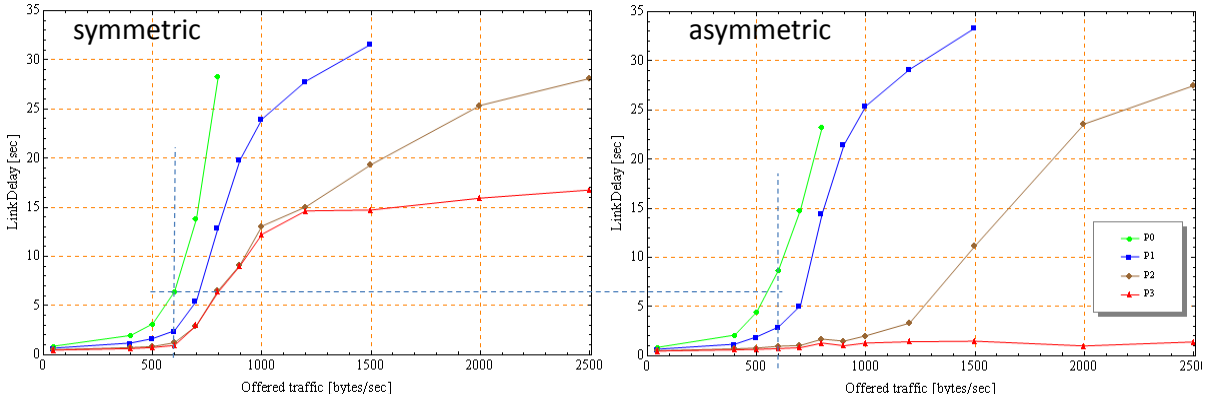

Figure 3.9 AHAn25 link delay [sec].

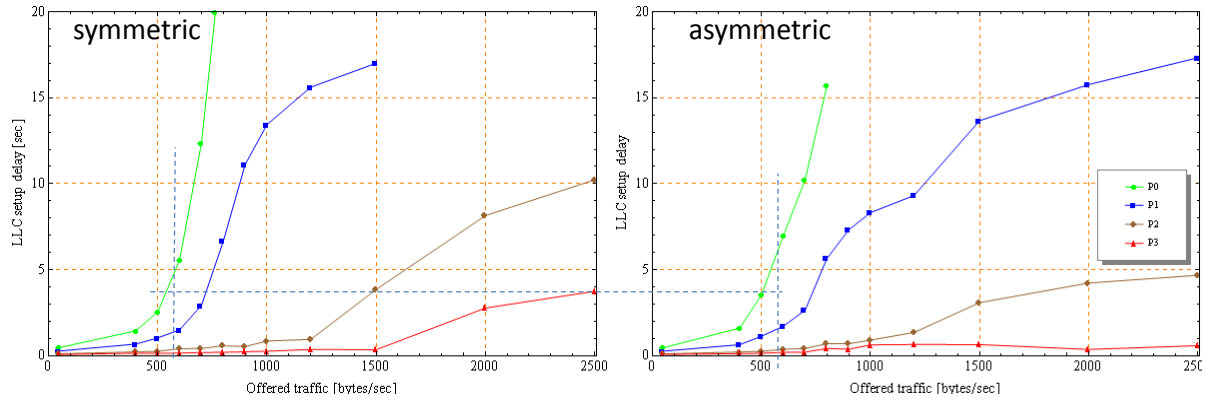

Figure 3.10 AHAn25 LLC connection setup delay [sec].

[8] The NBWF MLPP service does not implement pre-emption, and only one packet can be under service in the link layer at a time.

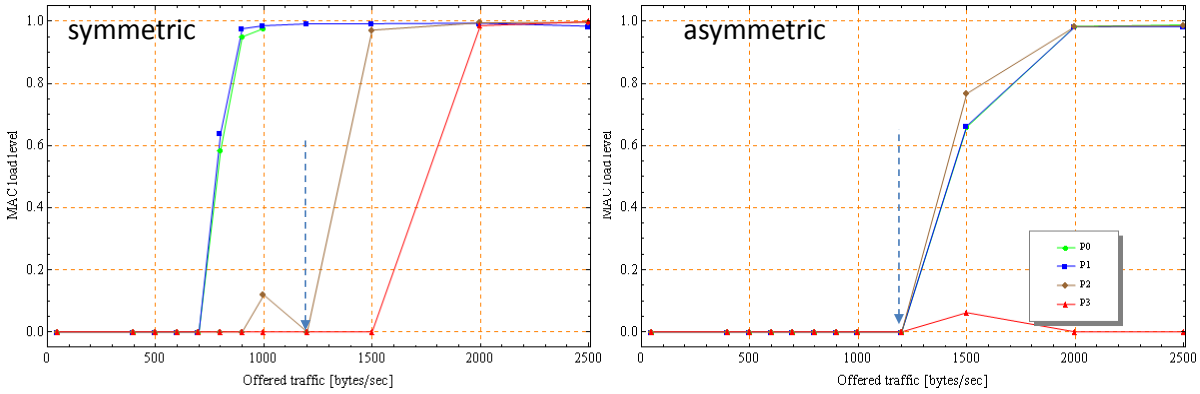

Figure 3.11 AHAn25 MAC load level.

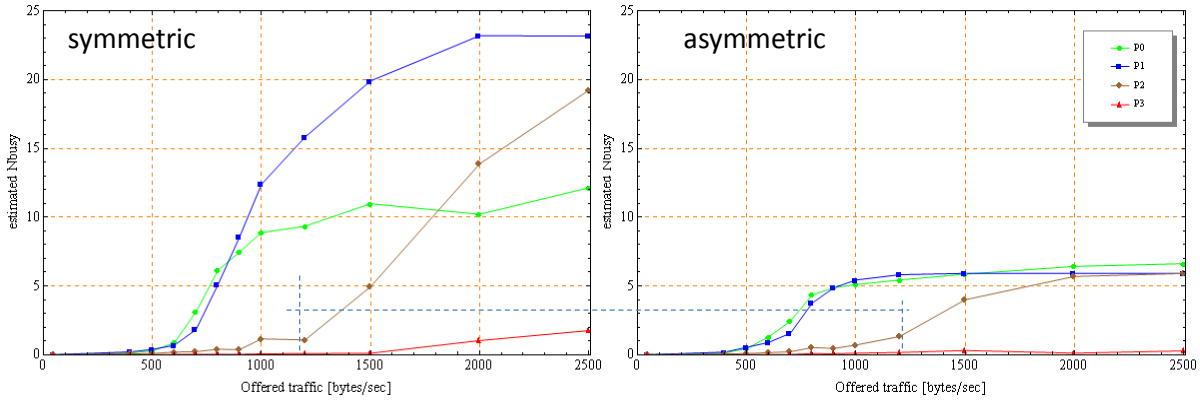

Figure 3.12 Estimated number of busy nodes (N_{busy}) based on MLL-reports.

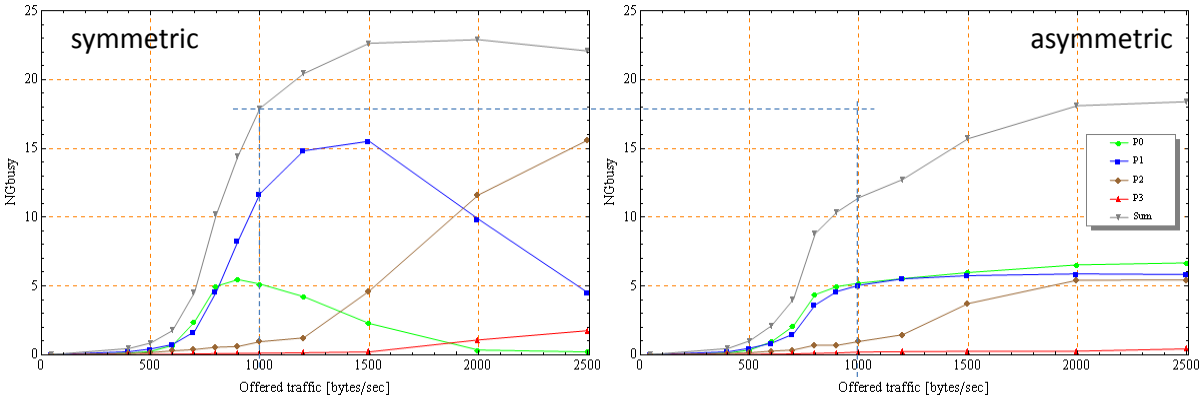

Figure 3.13 Simulated N_{Gbusy}

3.3 Lesson Learned

MAC parameter optimization is a lengthy process that demands many simulation runs. Generally, we are satisfied with the final results since both the symmetric and the asymmetric networks had good throughput conformity with the design goal. With regard to the end-to-end delay performance, less conformity was achieved; especially for the symmetric network due to the fact that MAC does not implement pre-emption of low priority traffic. Despite this, we do not recommend implementation of a pre-emption function.

By introducing the dimensioning rule “keep the collision rate less than 20%”, we have omitted the stage that shall consider the packet collision probability versus the channel idle period by simulating a set of different random access delays. When optimizing for the NBWF STANAGs, this stage must be done carefully and we should maximise the throughput for the MAC CR PDU.

The LLC connection establishment delay fluctuation between the priority levels is large (Figure 3.9). Some of the simulation experiments discovered a significant number of packet lifetime expiry at the LLC layer. Today, the LLC and the 3a layers use a common service lifetime threshold (“do not serve this packet if older than x seconds”) [2, chapter 5] for all the priority levels. LLC and 3a should implement a separate threshold value for each priority level.

4 GridN*n* at 50 watt

The purpose of this chapter is to analyse MAC protocol robustness as the number of nodes increases in a fully connected network. Figure 4.1 shows a Gridn100-network where the nodes send at 50W. According to the terminology used earlier, this network is identical with an AHAn100-network. A properly configured MAC protocol avoids most collisions regardless of the number of nodes. However, this chapter uses the MAC parameters optimised for the AHAn25-network in chapter 3. Here we are going to stress the MAC protocol by increasing the number of nodes. The playground size is kept fixed, while the number of nodes on the playground is varied. We are therefore guaranteed to simulate AHAn*N*-networks.

The network sizes considered are {16, 36, 100} [number of nodes]. In the AHAn100-network, the difference in received power between the links is up to 44 dB; the received power on the links 0→99 and 98→99 are -113.9 dBm and -69.7 dBm, respectively. In Figure 4.1, any transmission from node 98 will always destroy a captured packet on the link 0→99.

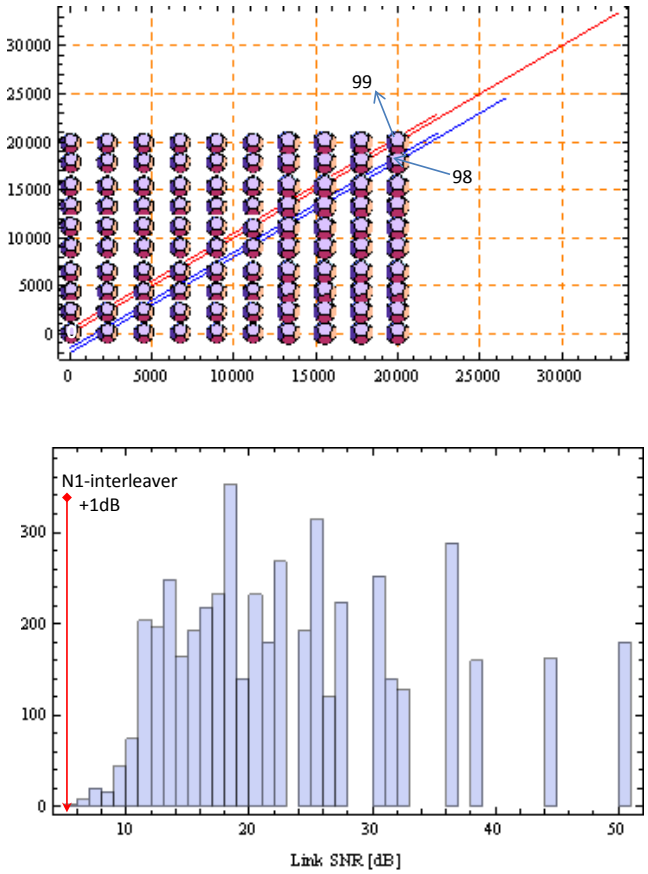

Figure 4.1 The GridN100 network on the 20x20 km^2 playground is shown in the upper picture. The picture below shows the histogram for the link SNRs.

A histogram for the link SNRs is shown in Figure 4.1, where the N1-interleaver SNR threshold is marked. Poor radio coverage is of no problem in this network. However, the diagram tells us that the QoS fluctuates significantly between the links when packet collisions occur, and we should divide the link statistics into groups. But this is a practical problem. The GridN100-network has $n \cdot (n-1)/2 = 100 \cdot 99/2 = 4950$ links. To conduct a simulation run that collects data from the weakest links {0↔99, 9↔90} separately, demands a simulation run length in order of days to achieve reasonable accuracy and confidence. Only the overall network statistics are therefore presented.

Figure 4.2 shows the throughput/delay-plots for the three networks and they differ little in the steady-state area (Λ<650); 650 bytes/s at 3-4 seconds link delay. The data transfer phase and the disconnect phase are not affected by the network size. However, we may have a small dependency because the connection establishment phase affects the remaining packet lifetime and this again may affect the data transfer phase. For example, a packet lifetime expiry during the data transfer phase leads to disconnection.

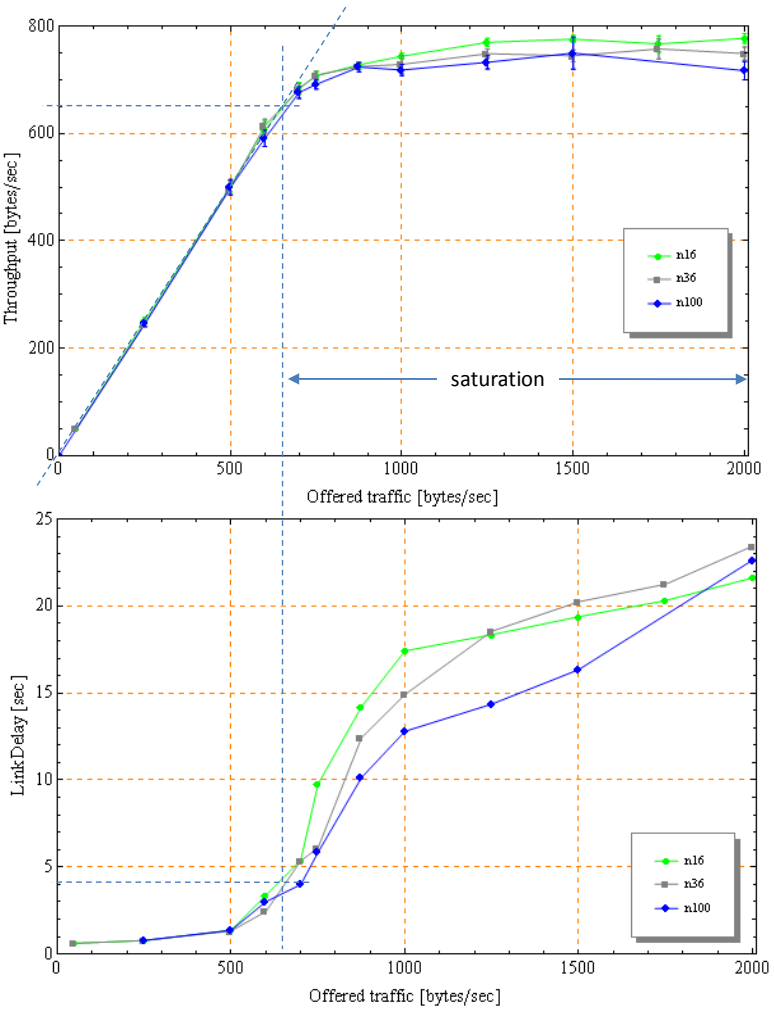

Figure 4.2 AHAnN throughput and delay performance. Both plots as 90% confidence intervals (simAug1abc).

A small network operates with longer channel idle periods than a large network, but a large network has a higher CR PDU collision rate, which can be seen in Figure 4.3. However, the p_{CC} is not alarmingly high. Note that this plot represents the average over all four priority levels.

Under the traffic conditions used in this chapter, a large network has less offered IP traffic per node than a small network. Therefore, a small network has longer input queues and then higher queue delays. On the other hand, a small network operates with lower LLC service times as illustrated by the lower plot in Figure 4.3.

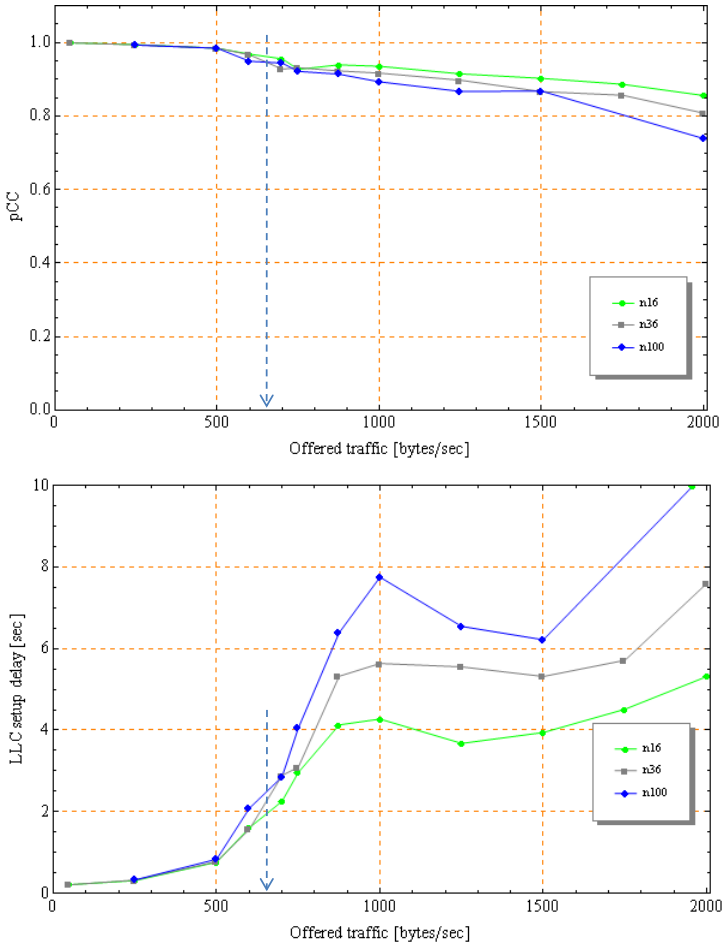

Figure 4.3 p_{CC} *and LLC setup delay for the AHAnN-networks. Sampled average values over all four priority levels without confidence control.*

4.1 MLPP Performance

In this section, we increase the detailing level by looking at the performance per priority level. Here we presuppose that the reader is familiar with reference [1, chapter 5 ”Multilevel Priority Networks”]. To save space, the performance plots for the GridN36 network are not included. Figure 4.4 presents the MLPP throughput plot and both plots are as expected. A larger difference is observed for the p_{CC}–statistics in Figure 4.5. p_{CC} becomes nearly 0.6 in the AHAn100 network; a significant amount of transmission capacity is consumed by the MAC CR PDUs. At Λ=1500 bytes/s both P1 and P2 use high-load scheduling. To decrease the p_{CC}, we must increase the MAC high-load level random delays. This is an easy task but will not be attempted here since NBWF shall not build network as large as 100 nodes.

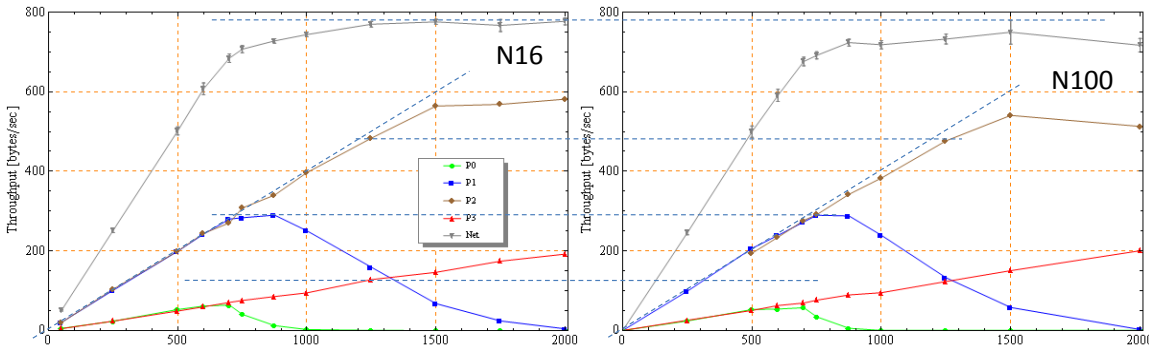

Figure 4.4 Throughput comparison between the AHAn16- and the AHAn100-network.

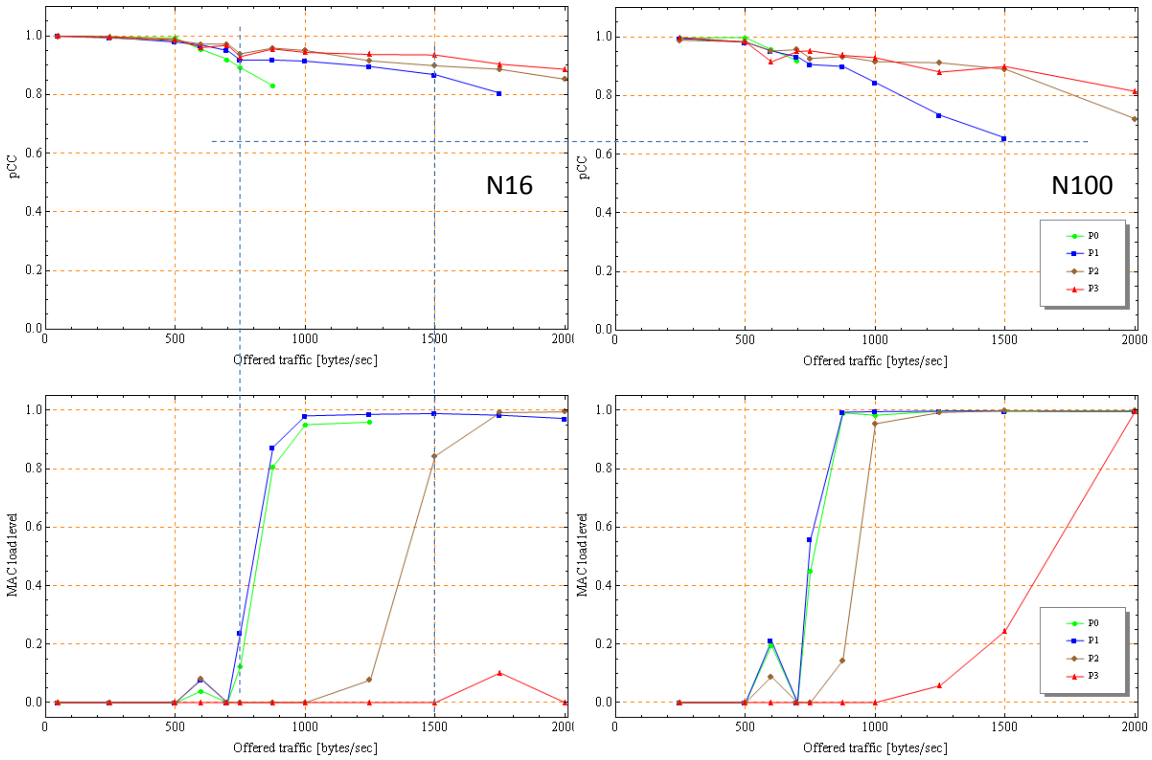

Figure 4.5 pCC and MAC load level comparison between the AHAn16- and the AHAn100-network.

4.2 Lesson Learned

As the number of nodes increases in an AHAnN-network, we surmise that it is the routing traffic that would crack a large network, and not the MAC protocol. Even though we simulated a large AHAn100-network using MAC parameters optimised for an AHAn25-network, the AHAn100-network showed good stability; the MLPP service behaved as it should, the throughput capacity was good and the signalling traffic was not alarming high (p_{CC} had an acceptable value).

5 GridN100 Networks

The previous chapter compared AHAn16 and AHAn100 networks and showed that the MAC protocol managed to stabilise even a 100-node network. 100 nodes form a much larger network than we expect for a real NBWF scenario. In this chapter, we push the limit further by reducing the network connectivity and analyse the connection setup phase and data the transfer phase. A GridN100-network where "all-hearing-all" is an AHAn100 network.

All the nodes are kept at a fixed location, as illustrated in Figure 5.1. Topology changes are achieved by selecting the transmitters' power levels from the set: {10W, 5W, 1W, 100mW}. Figure 5.1 shows that 10W gives a slightly degraded mesh topology, while a power reduction to 100mW leads to bad connectivity and many hidden-nodes. Since we use an all-to-all traffic pattern, the 100mW network has to serve a larger number of multihop routes than the 10W-network. Figure 5.2 visualises the SNR conditions on the network links. The 100mW network has a majority of the links at the wrong side of the N1-interleaver threshold.

Table 5.1 states the traffic generator settings used in this chapter. Use of multilevel priority traffic makes it difficult to analyse the simulation results, so this chapter resorts to single level traffic at priority P1. Note that the traffic pattern is "all-to-all", which means that this is a multihop scenario. A routing matrix is created for each network before the simulation experiments are started.

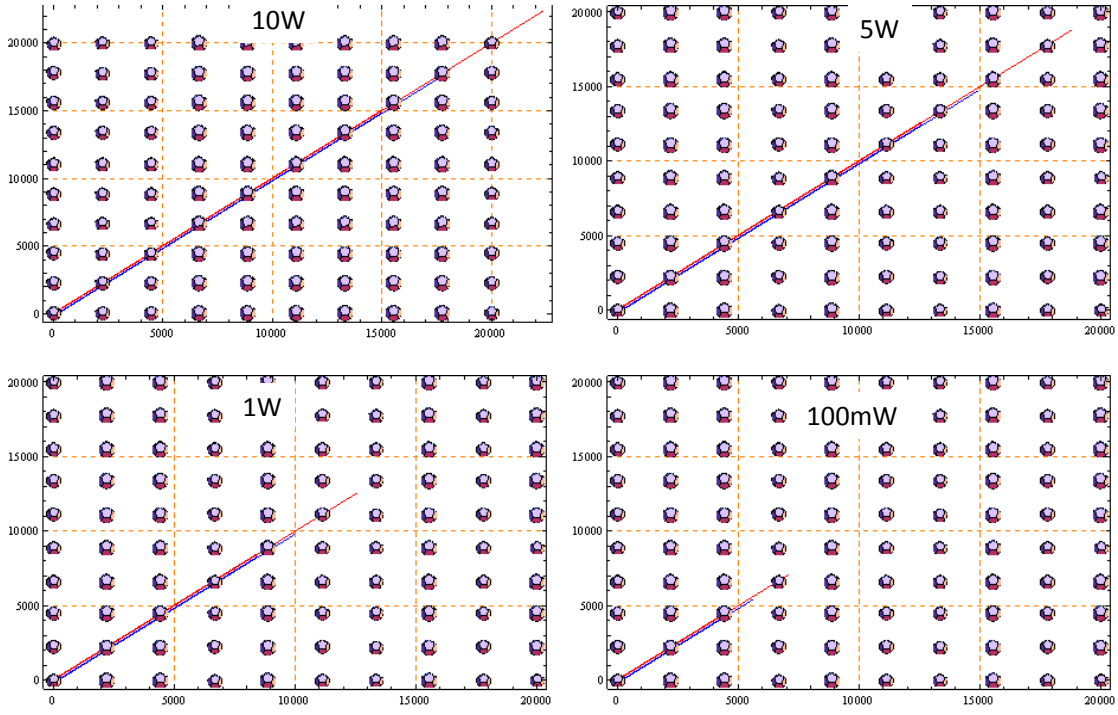

Figure 5.1 A GridN100 network in Egli "terrain" using the power levels {10W, 5W, 1W, 100mW}. 50W gives an AHAn100 network. The red and the blue lines mark the preamble and N1-interleaver ranges, respectively.

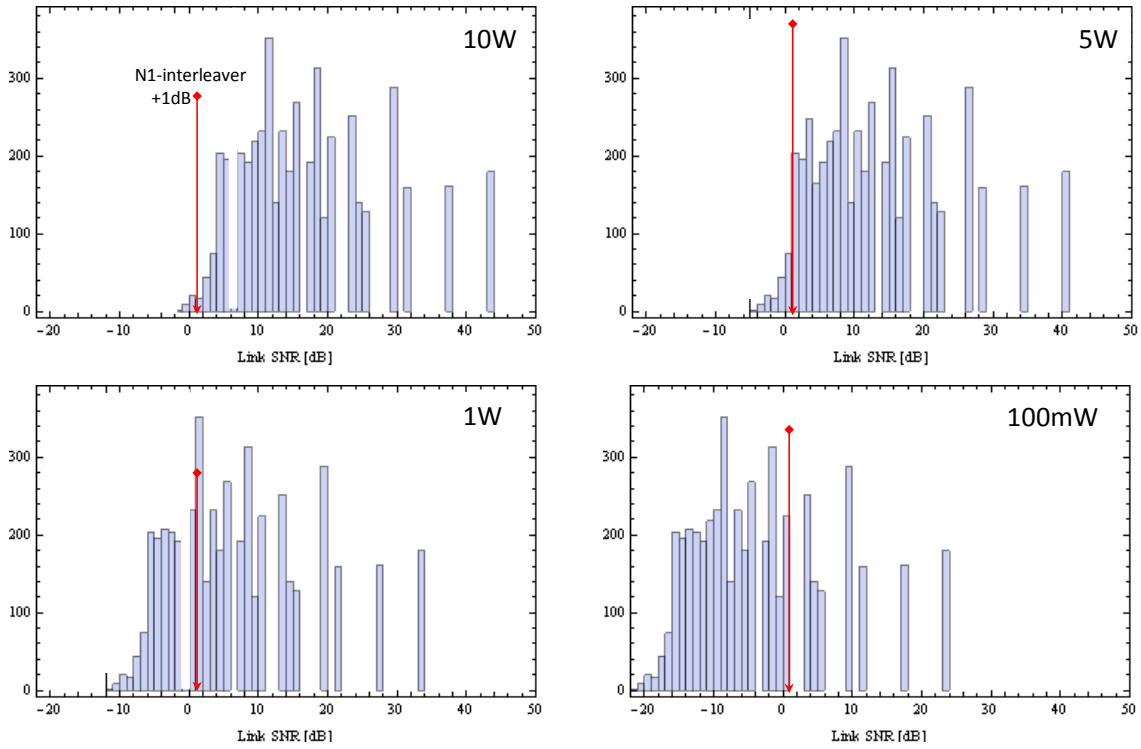

Figure 5.2 Histograms for the link SNR.

Parameter name	**Value**
Packet arrival distribution	Poisson
Packet length (layer 7)	Fixed 500 bytes
Priority distribution {P0(lowest),...,P3}	{0,1,0,0}
Traffic pattern	Unicast random uniform “all-to-all”
Maximum packet lifetime	60 seconds
Link ARQ	enabled

Table 5.1 Traffic generator parameters.

Figure 5.3 and Figure 5.4 present the simulated throughput/delay results for the four networks with reduced radio coverage. To have a reference performance (green lines), the results for the AHAn100/50W-network is included. At 50W, the performance is 600bytes/s@7sec (notation: throughput capacity @ end-to-end delay). As the power drops to 10W, the performance drops to 300 bytes/s @ 5sec. Power levels below 5W give a network with very low capacity. As the network becomes more fragmented, a number of factors contribute to degraded performance:

- The hidden-node problem increases the MAC CR PDU collision probability;
- Hidden-nodes cause MAC CC PDU losses;
- Hidden-nodes may interfere with an established MAC connection when they fail to register a successful TDMA reservation phase; and
- A part of the traffic is relayed over more than one radio hop, which consumes more transmission capacity than single-hop traffic.

Figure 5.5 presents the average number of radio hops (n_{hops}) travelled before reaching the end-destination. As it should, the 50W-network has $n_{hops} = 1$ regardless of the load levels. This in contrast to the 100mW-network, which starts at $n_{hops} = 1.5$, and decreases to near one with increasing load. As the load level increases, more IP packets are deleted due to lifetime expiry and only single-hop traffic is able to reach the end-destination (the packets must reach the end-destination to be included in the n_{hops}–estimate).

In NBWF, the major challenge in the connection setup phase is to send the MAC CR PDU without having a collision. The previous analyses have shown that NBWF protocols have a good efficiency in AHA-networks, but we know that the efficiency decreases as the number of hidden nodes increases. Section 5.1 analyses the connection establishment phase.

After the MAC layer has established an MAC connection, the other nodes should not interfere during the LLC SDU transfer phase, i.e., any packet losses during this phase shall only be caused by background noise on the radio channel. However, in networks with hidden-nodes, some nodes might be unable to register that a channel reservation has been completed successfully and start to send in a reserved TDMA slot . Section 5.2 below analyses the data transfer phase.

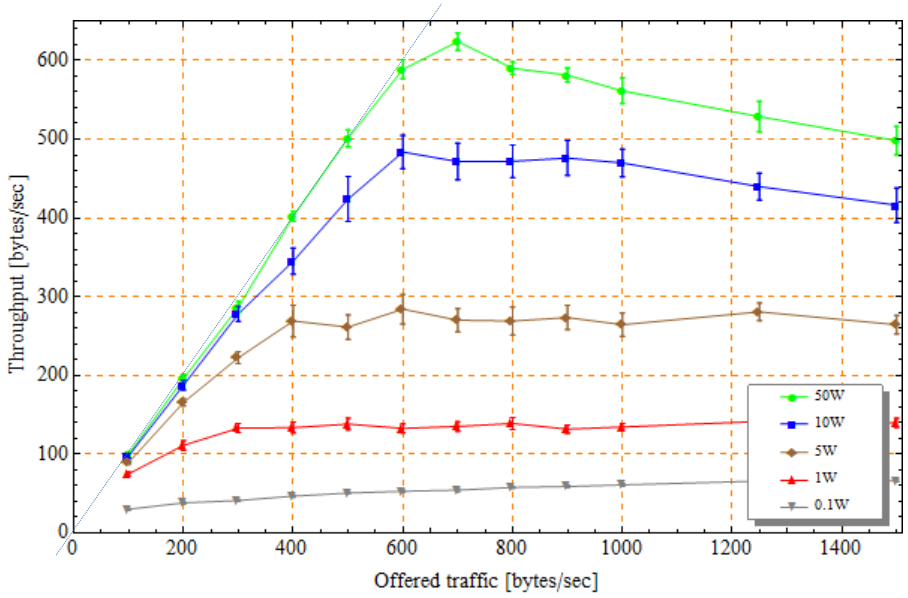

Figure 5.3 Simulated throughput vs. offered traffic (july31).

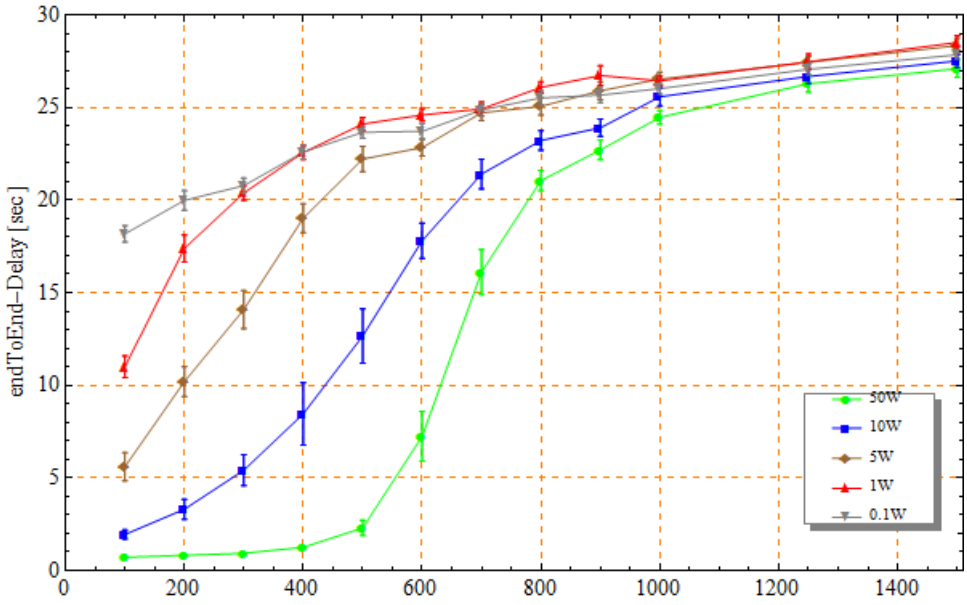

Figure 5.4 Simulated end-to-end delay vs. offered traffic (july31).

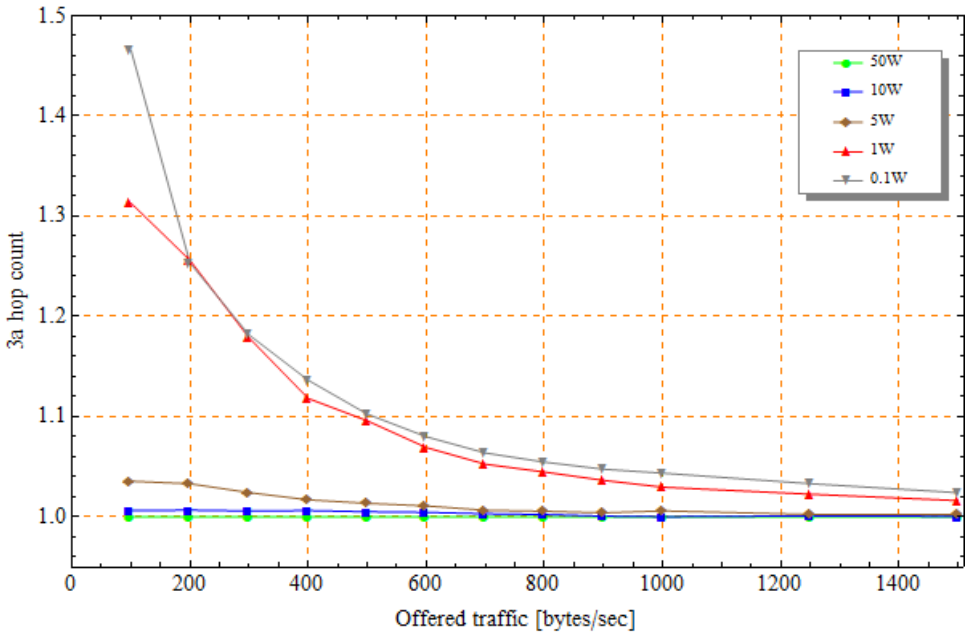

Figure 5.5 Network layer hop count.

5.1 MAC Connection Establishment Phase

The MAC reservation protocol uses a random access protocol during connection setup. The p_{CC}-estimator is a good indicator of how successful this phase is since it measures the MAC CR PDU success rate. Figure 5.6 shows that the 50W-network has low failure rate (say less than 10%) in the steady-state (offered traffic less than 600 bytes/s) but fails frequently at maximum load. The problem here is that the MAC random access parameters are optimised for a smaller network.

The topology conditions in the {5W, 1W, 0.1W}-network are too demanding for the MAC reservation protocol because p_{CC} is very low even at a low load level. The average number of

LLC CR-recovery attempts is also plotted in the figure. Note that this curve has a negative slope for power levels smaller than 5W. Consider the 100mW-network at the load level $\Lambda = 100$ bytes/s. At this point, the LLC connection setup delay is approximately 18 seconds (see Figure 5.7). Many recovery attempts are executed before the age limit is reached. When the traffic increases to $\Lambda = 1500$, the MAC connection setup delay is approximately 30 seconds. p_{CC} has decreased further and more nodes compete for access. Each recovery cycle takes a longer time and the lifetime control function deletes the LLC SDU before N_{crr} reaches a high value. LLC CO-setup delay statistics and N_{crr}-statistics are also collected for LLC SDUs that reaches the age limit.

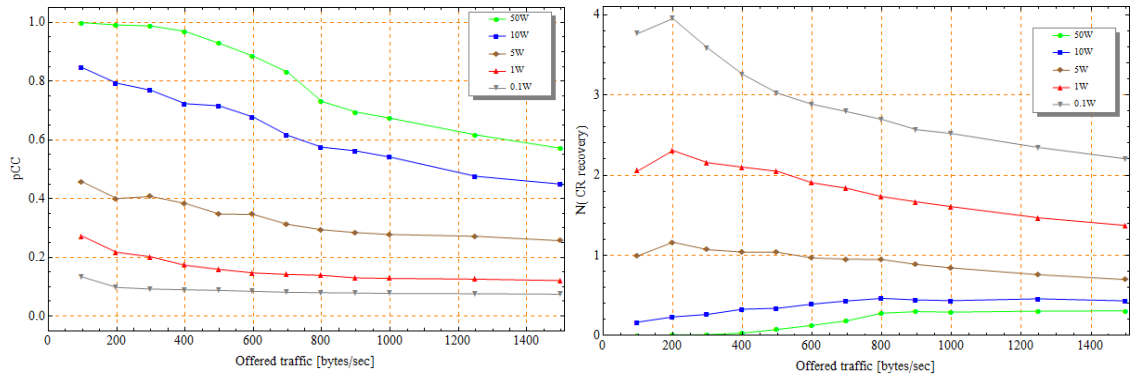

Figure 5.6 Simulated p_{CC} and N_{crr}.

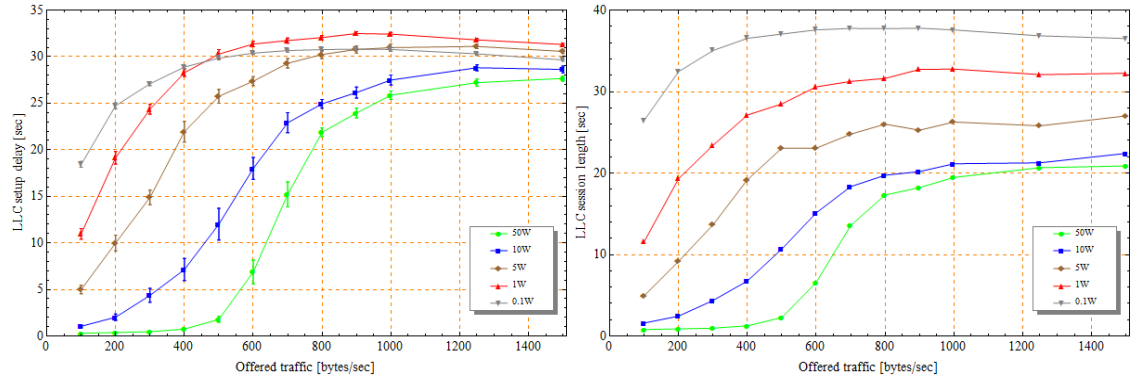

Figure 5.7 LLC setup delay (left) and LLC session length.

5.2 Data Transfer Phase

A successful MAC reservation phase should give a MAC-connection free from interference from the other nodes. This is the case for the 50W-network, which is an AHA-network. The other networks suffer from the hidden-node problem, some nodes may from time to time fail to register a successful reservation.

Our scenario is a radio scenario without background noise and any retransmissions of LLC DT PDUs must be caused by interference from the other nodes during the data transfer phase. Figure 5.8 presents the LLC retransmission ratio (N_{retx}) versus the offered traffic. As expected, the 50W-network needs not to retransmit ($N_{retx} \approx 1$). An acceptable retransmission rate is experienced in

the {10W, 5W}-networks. It is interesting to note that the retransmission rate is nearly flat, that is, not affected by the offered traffic, but no confidence control is applied to this estimator!

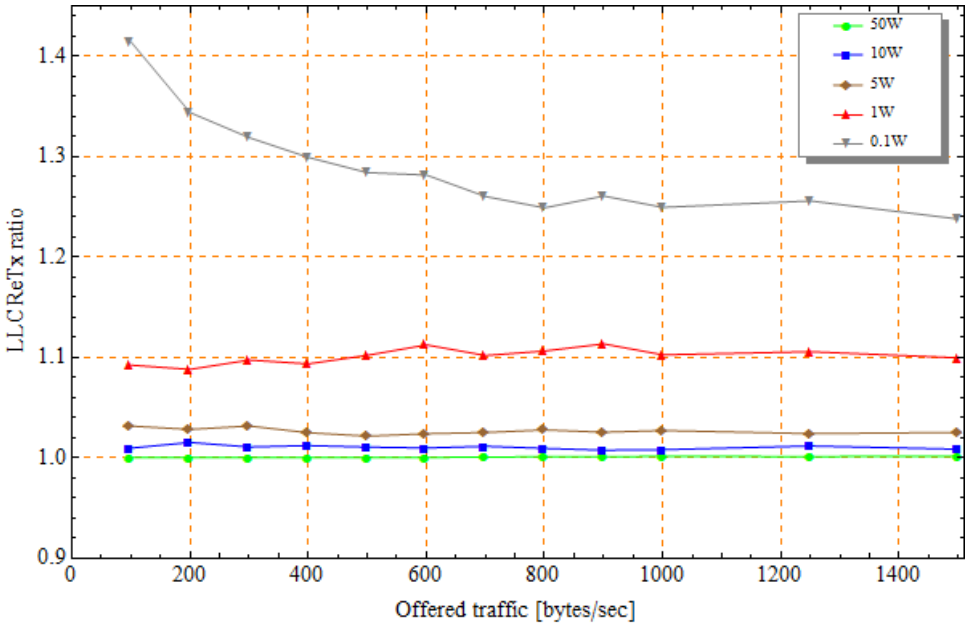

Figure 5.8 LLC retransmission ratio.

5.3 Adaptive MAC Scheduling

With the intention to estimate the network load level, NBWF shall measure the number of busy nodes (N_{busy}) as explained in reference [1, section 6.3]. Any error in the N_{busy}-estimator will give underestimation or overestimation of the network traffic level with the negative effect of using inferior MAC random access parameters. The NBWF simulator can estimate the number of busy nodes in a network ($N_{G,busy}$) perfectly. A node does not interfere with the nodes more than two-hops away and the 100mW-network may have a gain of spatial reuse.

Figure 5.9 compares $N_{G,busy}$ with N_{busy}. We observe a good tracking of the load levels at the power levels {50W, 10W, 5W}. The MLL-report does only include information about the load state as observed by the sending node and therefore results in underestimation of the number of busy nodes in a fragmented network. The figure shows that we have a significant underestimation of the number of busy nodes in the {1W, 0.1W}-networks. This is not a design flaw since the adaptive MAC scheduling is not meant to be a cure against the hidden-node problem.

Based on the N_{busy} –samples, the MAC protocol shall select one of two random access parameter sets per priority. A random delay is added to the MAC CR PDUs only. Figure 5.10 presents the MAC CR load level versus offered traffic. Here we see that the 50W-network uses short access delays for offered traffic below 400 bytes/s. Then the 50W-network uses long access delays more frequently. When the offered traffic becomes higher than 700 bytes/s, the long access delay is always used. It is the 1W-network that switches to a high-load MAC scheduling state first. At $\Lambda = 200$ bytes/s, the $\{50W, 10W, 5W, 1W, 0.1W\}$-networks have the ordered set $N_{busy} = \{0.1, 0.9, 4.0, 7.1, 3.5\}$.

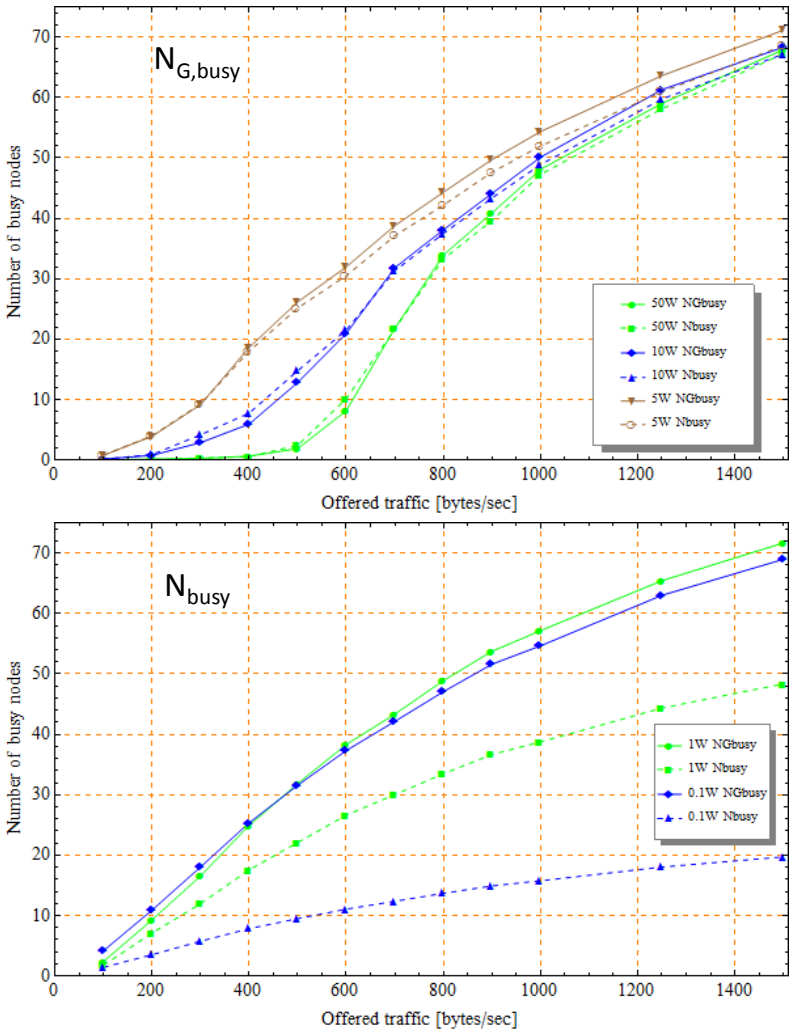

Figure 5.9 Number of busy nodes $N_{G,busy}$ (the correct average) and N_{busy}(the estimated average).

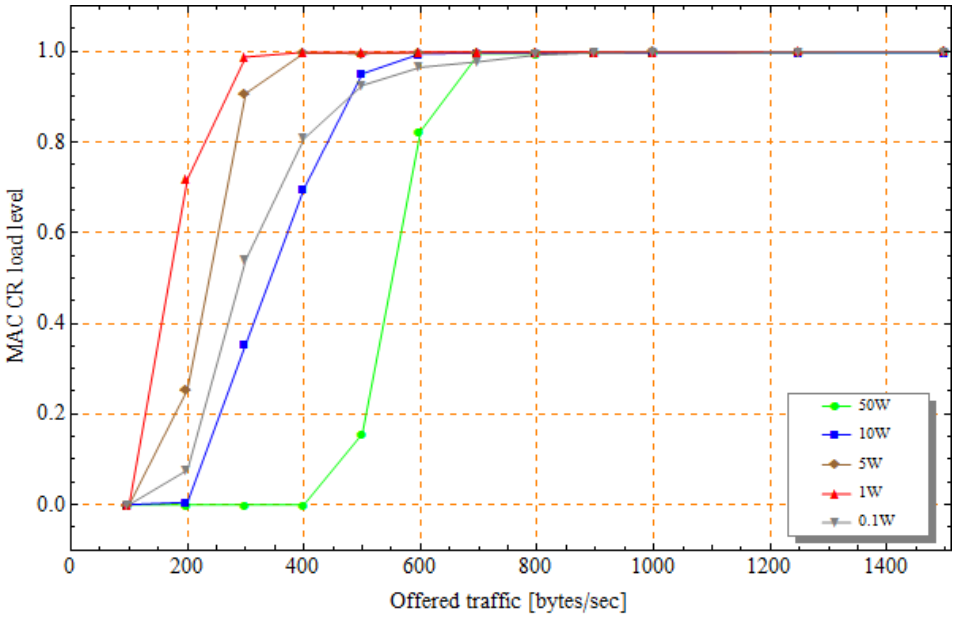

Figure 5.10 MAC CR load level.

5.4 The Impact of the LLC NegExp Backoff

Packet collision on the radio channel may lead to loss of MAC CR PDUs, but the MAC protocol does not implement recovery from packet loss. However, MAC issues a MAC-Disconnect.indication setting the reason-parameter to *MissingCC*. As explained in [2, chapter 7], LLC shall use a negative exponential backoff function during this recovery process. To estimate the efficiency of this function, we disable this function by allowing the LLC entity to issue a new connection request immediately after MAC signals a MAC CC PDU loss event.

Figure 5.11 and Figure 5.12 clearly show that the LLC negative exponential backoff improves the network performance. At low load levels, the 50W-network does not get improved performance; throughput and end-to-end-delay are unaffected. But in saturation, the throughput performance becomes higher with backoff enabled. The other networks achieve lower end-to-end delays during low to medium traffic and improved throughput performance at higher loads.

Consider the 3a hop-count plot in Figure 5.13 and the 100mW-network. To be included in the statistics, a packet must reach its end-destination. At low load the backoff increases the hop count from 1.27 to 1.47, which means that more multihop packets arrive at their destinations. Also the 1W-network gets a hop count improvement by using backoff.

Even though the negative exponential backoff is designed to enhance the connection setup phase only (Figure 5.14), Figure 5.15 shows that data transfer gets a lower retransmission rate, which means that fever nodes are granted a MAC-connection simultaneously, or that a MAC-connection is less frequently hit by a MAC CR PDU.

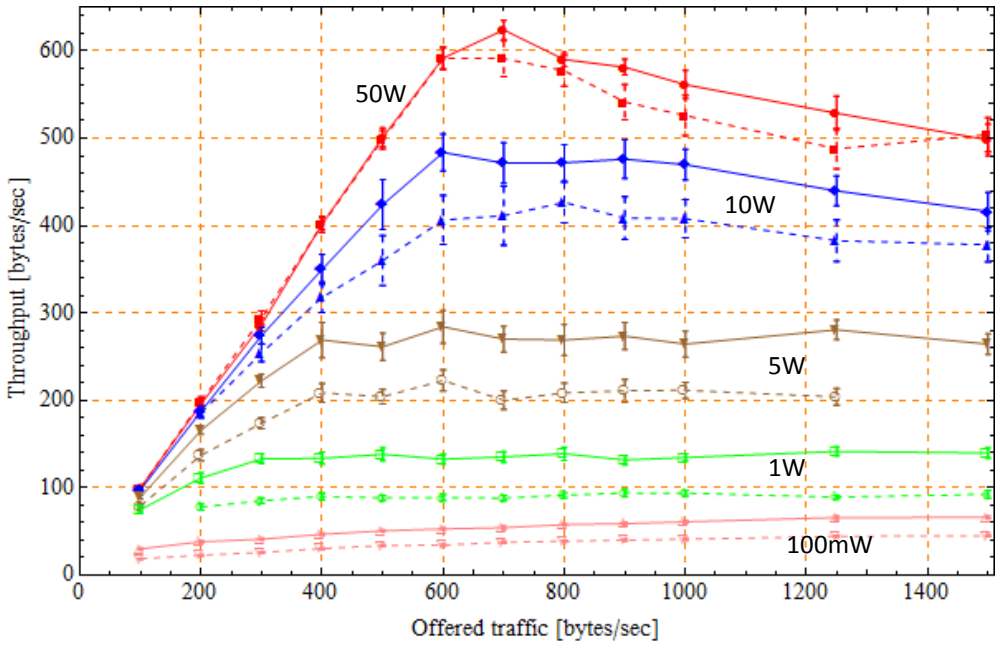

Figure 5.11 GridN100-throughput performance with negative exponential backoff (solid lines) and without (dashed lines) (simAug8).

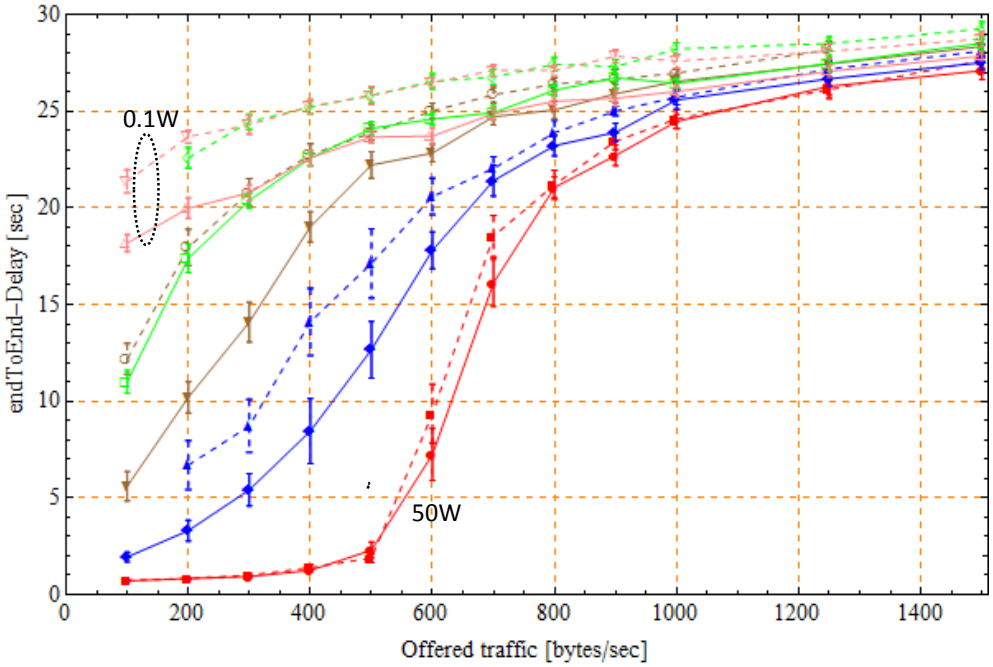

Figure 5.12 GridN100-delay performance with negative exponential backoff (solid lines) and without (dashed lines) (simAug8).

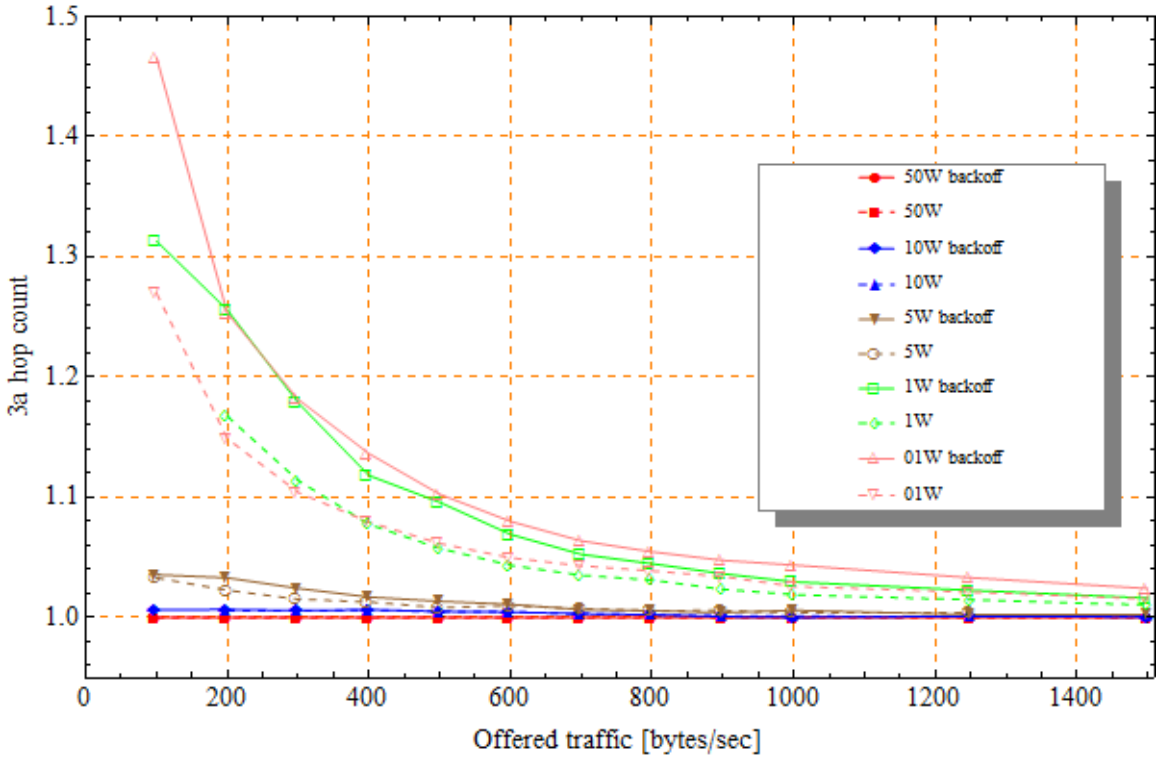

Figure 5.13 Average number of radio hops vs. offered traffic with (solid lines) and without (dashed lines) negative exponential backoff.

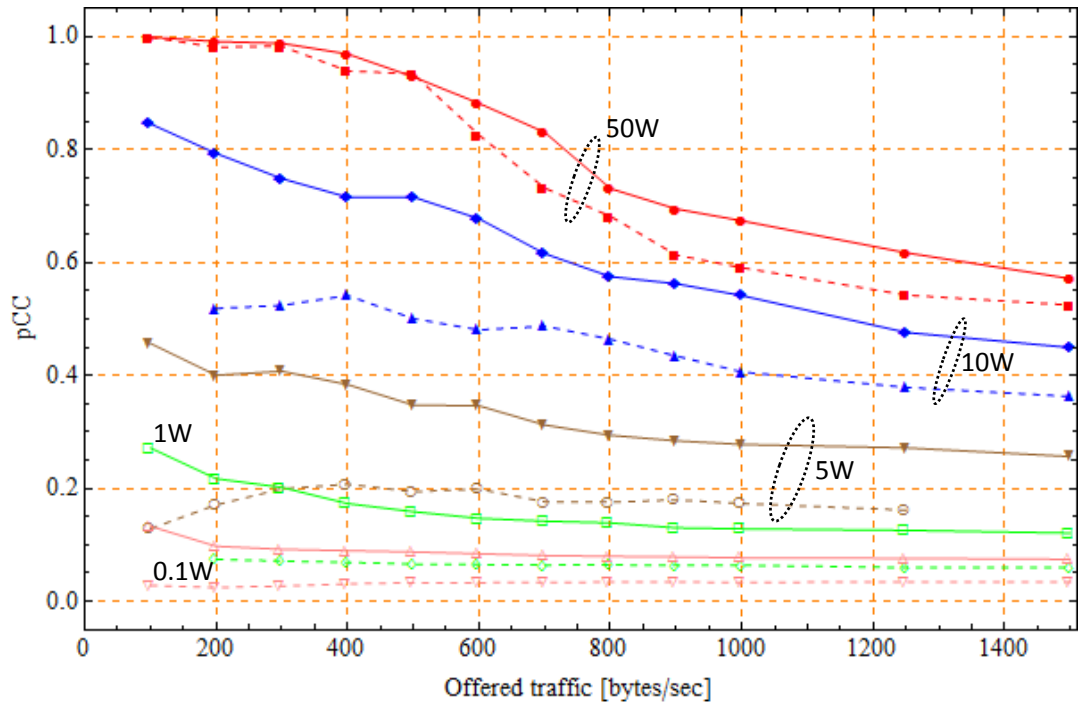

Figure 5.14 p_{CC}-performance with negative exponential backoff (solid lines) and without (dashed lines) (simAug8).

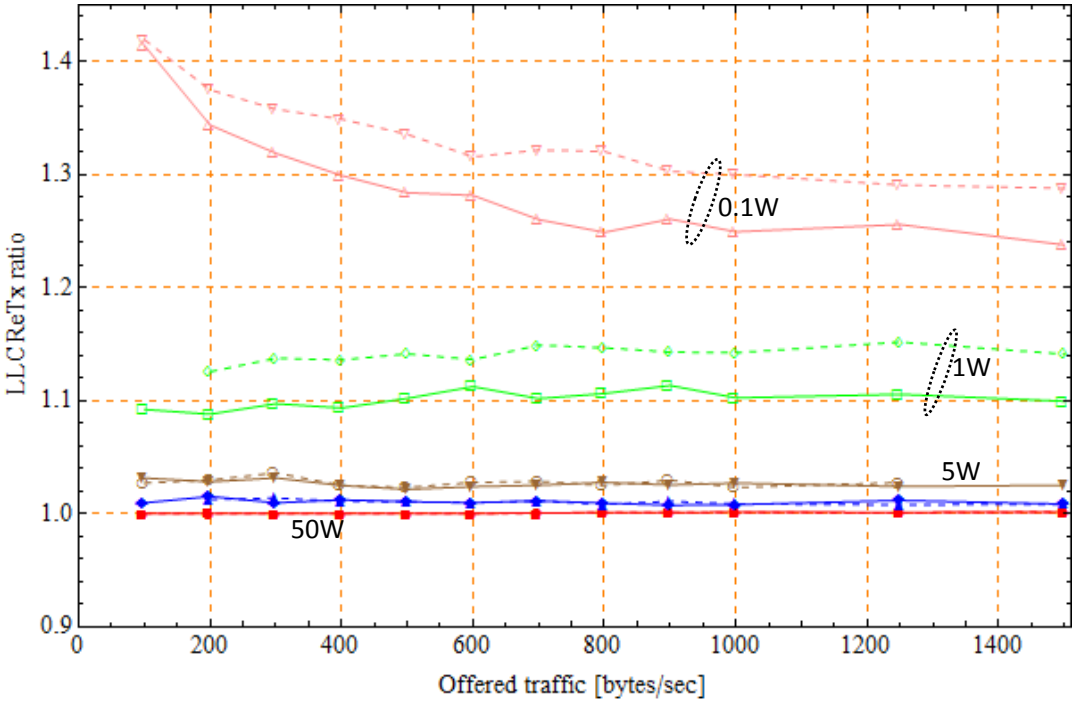

Figure 5.15 LLC retransmission rate with negative exponential backoff (solid lines) and without (dashed lines) (simAug8).

5.5 Lesson Learned

As an NBWF-network gets reduces radio coverage, it is the MAC reservation protocol that is the main contributor to degraded throughput. It is difficult for MAC CR PDU to succeed due to collisions. In the {5W, 1W, 0.1W}-networks, p_{CC} is low regardless of the load levels (Figure 5.6) and the LLC layer must execute many recovery attempts. Necessarily, this must lead to throughput degradation (Figure 5.3). When the LLC layer has got an MAC-connection, the MAC-connection seems to be robust since the retransmission rate is acceptable for all the networks, except for the 100mW-network.

The LLC negative exponential backoff function is not designed to be a cure against the hidden-node problem, but it relieves it. No signalling information across the radio channel is required and the software complexity is very low. Only positive effects were observed in the GridN100-network.

6 Packet Lifetime Control

All earlier simulation experiments have used network based packet lifetime control while the draft NBWF STANAG [8] specifies use of node based packet lifetime control. This chapter compares these packet lifetime control strategies. Below we specify how they operate:

Network based lifetime control (NetBlc)
The network guarantees a maximum packet lifetime in an NBWF subnetwork. The entry node inserts a lifetime value and the network nodes decrement this value as the packet is relayed towards its end-destination. If the lifetime expires in the network, the packet is deleted silently. To implement this type of lifetime control, a remaining lifetime field in the data packets must be included.

Node based lifetime control (NodeBlc)
The network does not guarantee a maximum packet lifetime in an NBWF subnetwork[9]. The entry node uses a local lifetime counter which is decremented as long as the packet is stored in the entry node. If the lifetime expires, the packet is deleted silently. This type of lifetime control requires no PCI-field in the data packets. When a packet arrives at a relay node, this node assigns a local lifetime value to the packet, regardless of its age, and operates exactly as the entry node.

Let t_{L0} denote the packet lifetime value set at layer 3a. In the simulator, the minimum remaining lifetime to be served at the network level is $t_{L0} - 3a::t_{Lmin}$ where $3a::t_{Lmin}$=15 seconds. Any packet is discarded if the packet has not left the 3a queue within $t_{L0} - 3a::t_{Lmin}$. Similarly, LLC layer also applies an age limiting procedure using the threshold $llc::t_{Lmin}$ = 10 sec.

[9] NBWF should implement a protection against infinite looping of packets. For example, use a hop counter.

6.1 GridN25

A GridN25-network using the transmitting power set {50, 10, 5, 1} watt is analysed in this section, see Figure 6.1. Power levels below 1 watt give too bad connectivity. The network based lifetime control function sets t_{L0} to 60 seconds, while the NodeBlc scheme uses the t_{L0}-set {60, 45, 30} seconds. When t_{L0} = 30, a packet cannot be queued for more than 15 seconds at layer 3a. By setting t_{L0} to a low value, multihop packets get a higher probability to reach the age limit before the end-destinations are reached. Less change in performance is expected from the NodeBlc since the IP-packets are assigned a new lifetime value by the relay nodes. NodeBlc guarantees a maximum residence time in a single node only.

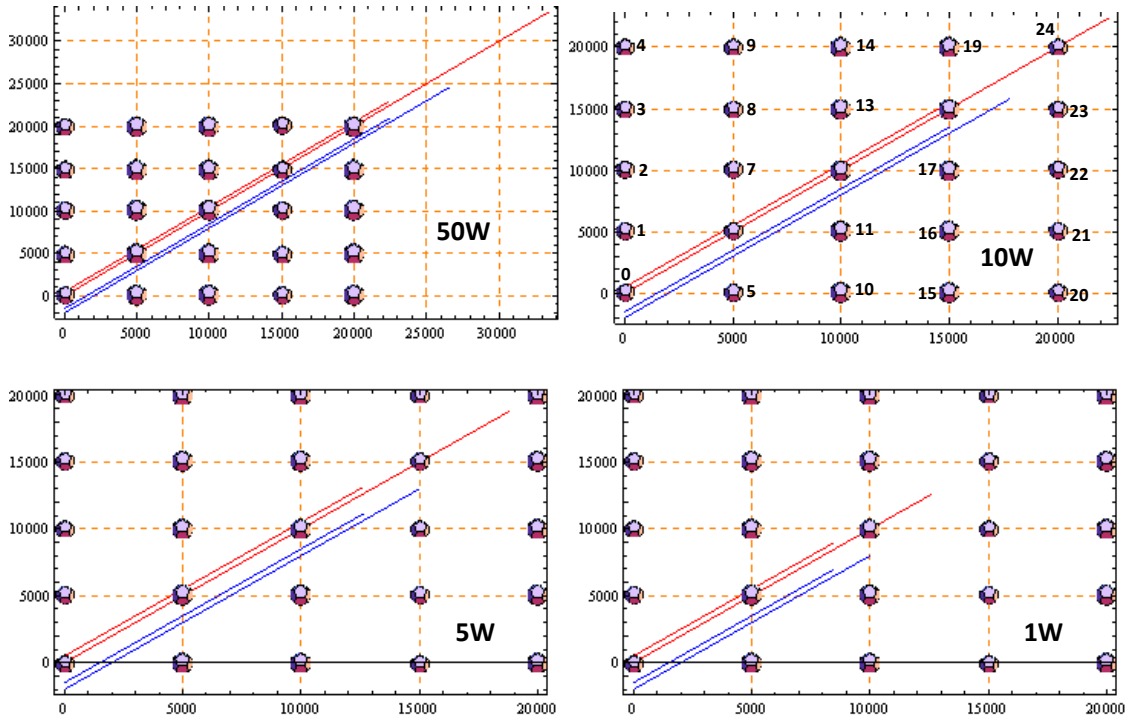

Figure 6.1 GridN25-network using the power set {50, 10, 5, 1} watt.

Figure 6.2 shows the simulated network throughput. Nodes located in the centre of the grid (e.g. node 12) have better RF-links to their neighbours than the corner nodes (e.g. node 20). Even though the throughput varies much between the locations for power levels less than 50W, the average throughput over all the nodes is measured only[10].

In the 50W-network, for t_{L0} = 60 seconds, both NetBlc and NodeBlc produced exactly the same data (this applies to all statistics, not only the throughput). Another result would indicate an implementation error since this is a single-hop network and both methods shall have identical behaviour. As t_{L0} decreases, more packets are deleted by the lifetime control function and the average 3a queue length decreases; in the 50W-network for t_{L0} = {60, 30} at maximum load, we have the average 3a queue size {4.2, 1.2} [number of packets stored].

[10] To collect statistics for a single IP-stream demands very long run times.

A power reduction from 50W to 10W gives a large drop in throughput despite that the radio coverage figure (Figure 6.1) does not indicate a large reduction in the RF connectivity. From Figure 6.3 we observe a significant decrease in p_{CC} while the 3a hop count stays near one. In the 10W-network, the MAC CR PDU packets collide more frequently, and it takes a longer time to establish a MAC connection. The LLC DT PDU retransmission rate is near zero (simulated results not shown), so the data transfer phase is modestly degraded by hidden-nodes.

Figure 6.4 shows that the end-to-end delay is more influenced by the lifetime control method than the throughput. NodeBlc30 achieves significantly lower end-to-end delays than NodeBlc60 and NetBlc60, which is not surprising since the former uses an age limit 30 seconds lower than the two others. In the 50W-network, the NodeBlc30 gives slightly lower throughput capacity than the three other schemes; $\lambda = 578 \pm 5$ versus $\lambda = 598 \pm 6$ bytes/s at $\Lambda = 600$, but the end-to-end delay is significantly lower at this load level compared to the results for NetBlc60 and NodeBlc60. NodeBlc30 is the best choice for all four networks.

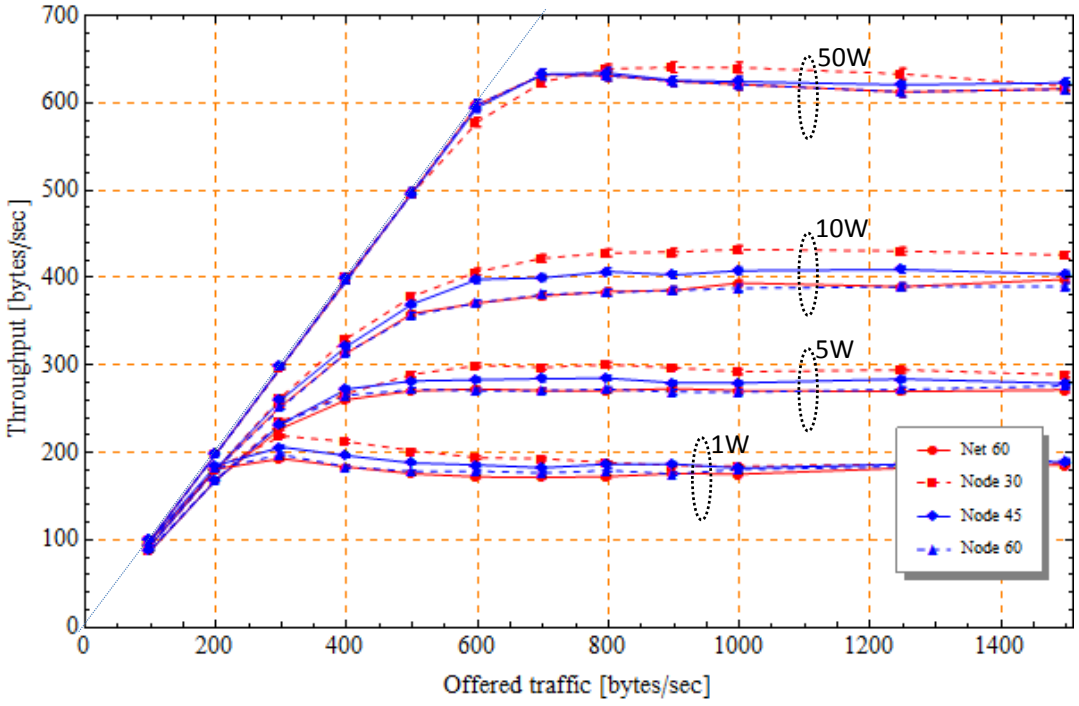

Figure 6.2 GridN25 simulated throughput. "Net 60" means network based lifetime control with lifetime parameter setting 60 seconds. "Node 45" means node based lifetime control using 45 seconds (simSept3).

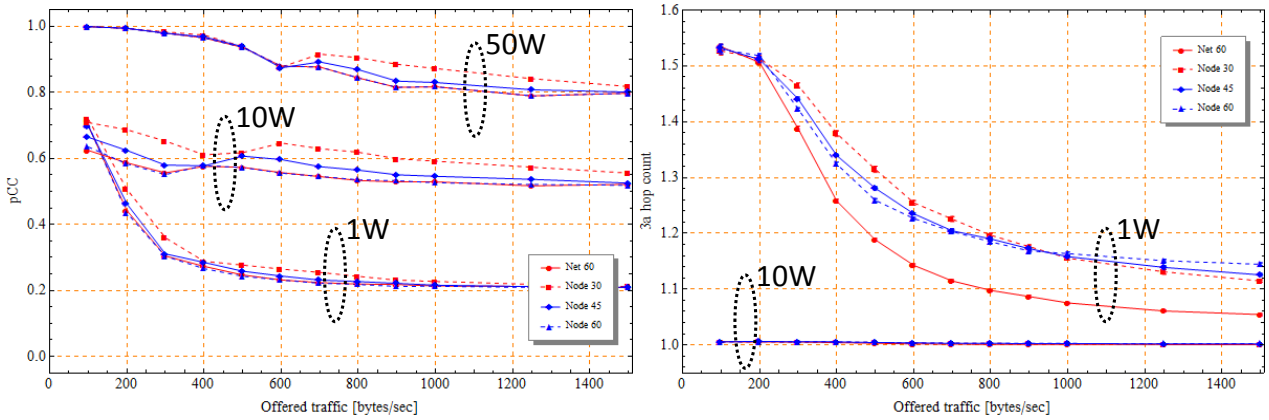

Figure 6.3 GridN25 simulated p_{CC} and 3a hop count.

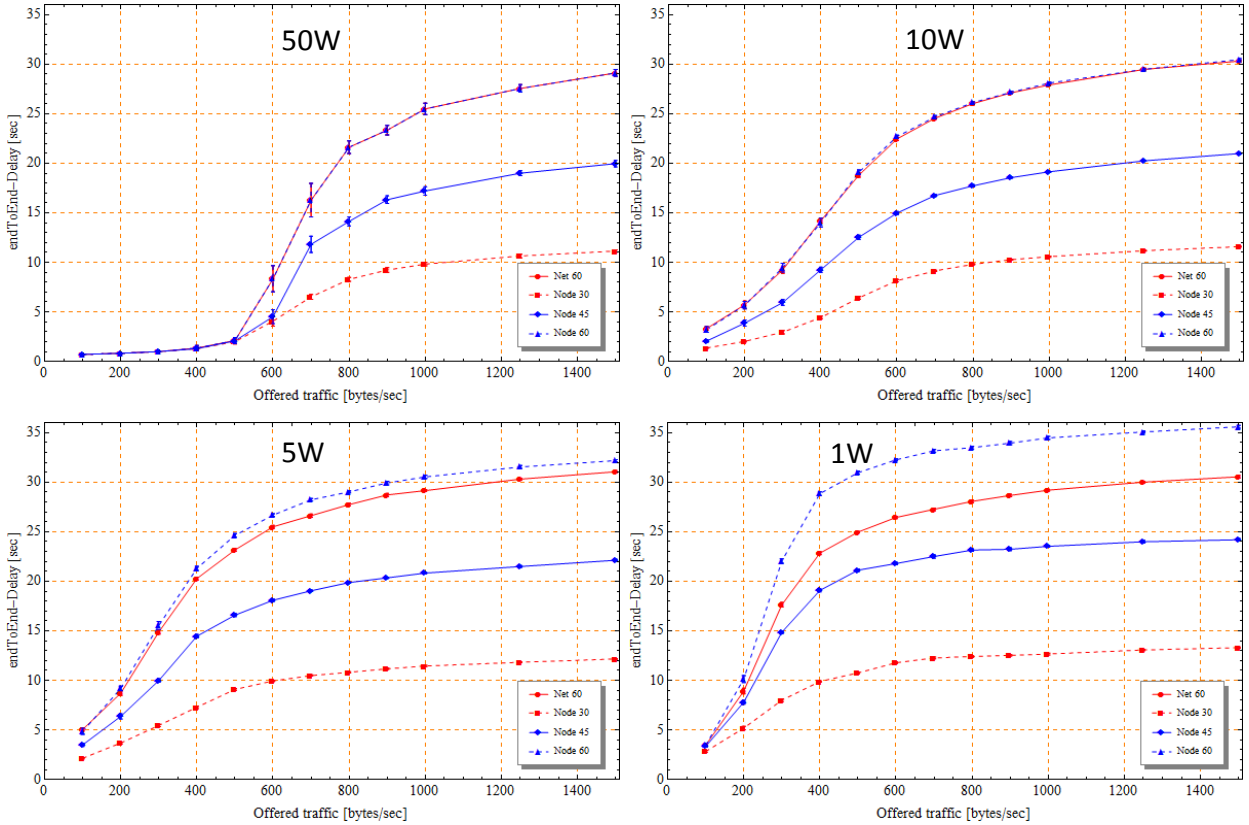

Figure 6.4 GridN25 simulated end-to-end delay.

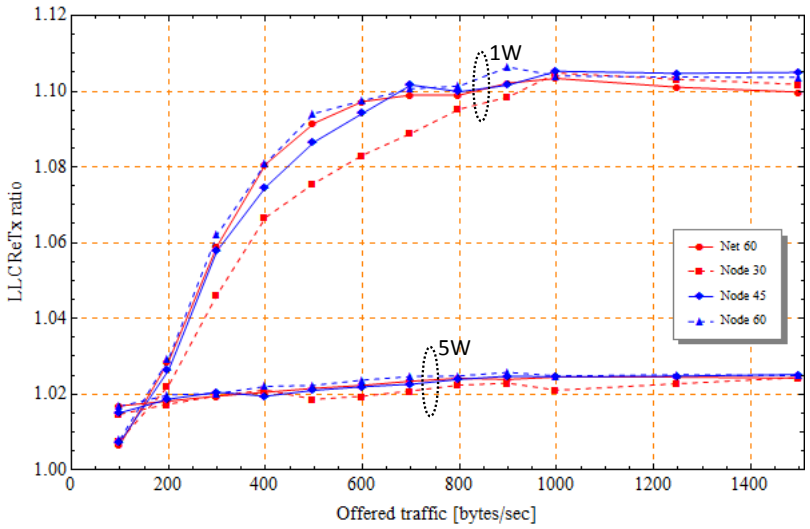

Figure 6.5 GridN25 simulated LLC retransmission ratio. A sample value of one means no retransmission.

6.2 GridN100

To challenge the NBWF protocols with a scenario they are not designed for, we repeat the simulation experiments using the GridN100-network presented in Figure 5.1. Figure 6.6 and Figure 6.7 present the simulation results. The discussion of the results and the conclusion given in the previous section also applies to the GridN100-network in this section.

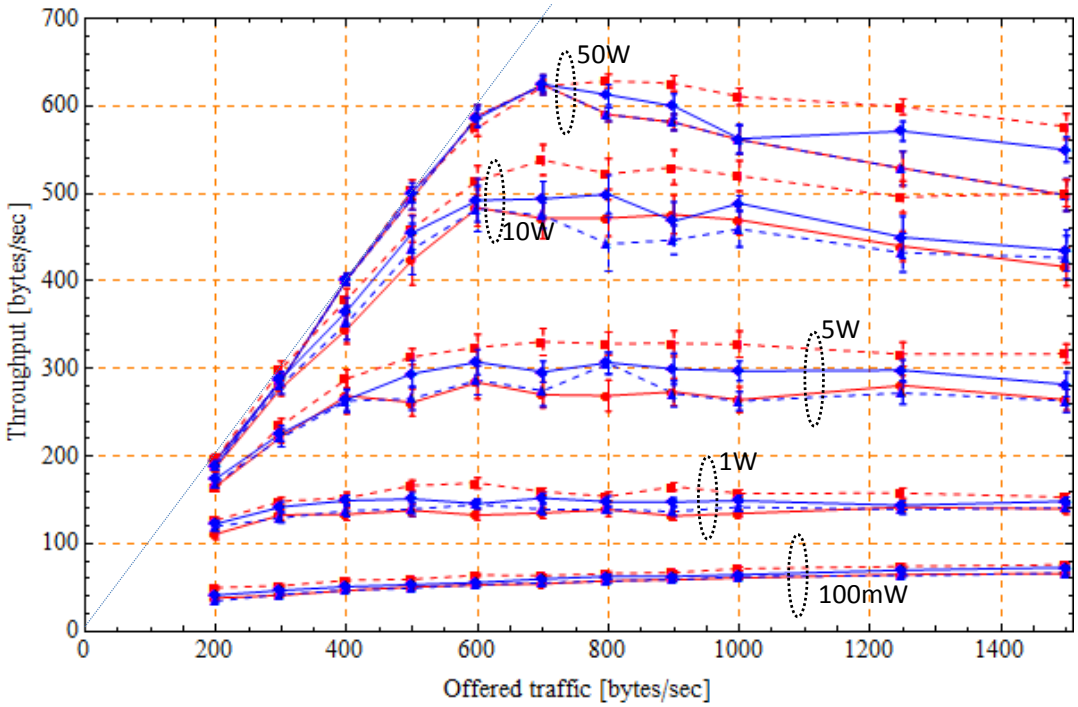

Figure 6.6 GridN100 simulated throughput (simSept4).

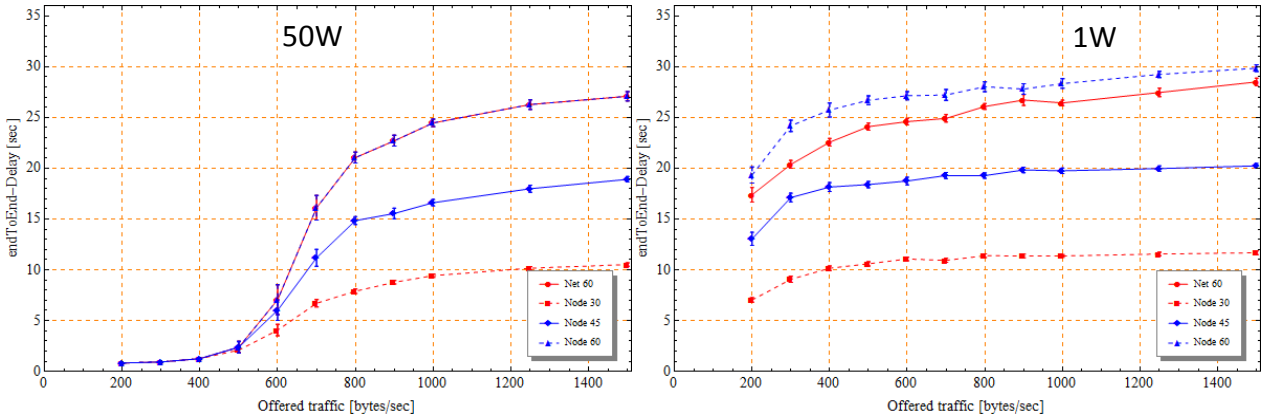

Figure 6.7 GridN100 simulated end-to-end delay.

6.3 Lesson Learned

We tested a GridN25-network and a GridN100-network using a set of different radio coverage scenarios. The NBWF protocols are not designed for a 100-node network, but the MAC protocol handled even this situation.

By reducing t_{L0}, the initial lifetime value, the networks experienced significantly lower end-to-end delays without throughput capacity degradation. By assigning a lower t_{L0}–value, more packets were deleted from fresh traffic input queues in the entry nodes, leading to decreased MAC offered traffic that again improved the performance. Node based lifetime control using $t_{L0} = 30$ seconds was the best choice. This chapter used 3a::t_{Lmin}=15 seconds and llc::t_{Lmin} = 10 sec. Simulation experiments with other values is a subject for further study.

7 Priority Handling in Multihop Networks

Earlier simulation experiments [1] showed that the MLPP service sorts the traffic as desired in all-hearing-all scenarios. All the layers in the NBWF protocol stack implements priority handling, but it is the MAC layer that allocates the radio channel and hence has the greatest impact, see [1, figure 6.5]. As a network turns from a fully meshed topology to multihop, the MAC protocol decreases its efficiency with respect to the priority sorting characteristics. The subject of this chapter is to analyse the quality of the MLPP service in multihop networks. Figure 7.1 presents the three networks to be analysed.

Both networks have two AHA-groups g1 = {0, 1, 2} and g2 = {3, 4, 5}; the g1-members send P0-packets to the g2-members, while the g2-members send P3-traffic (highest priority) to the g1-members. These two groups have no radio contact and the traffic must be forwarded by the intermediate nodes. At low load, the traffic travels across 3 hops and 4 hops in the MHn8 and MHn9 networks, respectively.

These networks have multihop traffic only. At low load levels, the distance covered should be 2, 3 and 4 hops, and when the load level increases, the hop-count (number of radio hops) should decrease due to packet lifetime expiry[11]. This is confirmed by the 3a-hop-count plot in Figure 7.3.

What throughput performance should we expect? Both networks have 6 nodes generating fresh traffic. By simulating an AHAn6-network (see Figure 7.4), we can calculate the throughput capacity upper boundaries as MHn7: $\lambda_{C,AHAn6}/2 = 300$, MHn8: $\lambda_{C,AHAn6}/3 = 200$ and MHn9: $\lambda_{C,AHAn6}/4 = 150$ bytes/s. $\lambda_{C,AHAn6}$ denotes the AHAn6-throughput.

Figure 7.2 shows the throughput performance. The priority sorting characteristics are still acceptable, but the highest priority traffic gets a falling slope when the network is loaded to high. This is typical shape for multihop networks and has nothing to do with the priority handling function.

Define the protocol efficiency β as the "measured throughput"/"calculated throughput". From the numerical values above we have $\beta_{MH7} = 280/300 = 0.9$, $\beta_{MH8} = 120/200 = 0.6$ and $\beta_{MH9} = 90/150 = 0.6$, which means that the protocol efficiency is the same in the two latter topologies. In the MHn7-topology, the MAC CC PDU operates as an effective cure against the hidden-node problem since a CC PDU sent by node number 6 is received by all other nodes in the network.

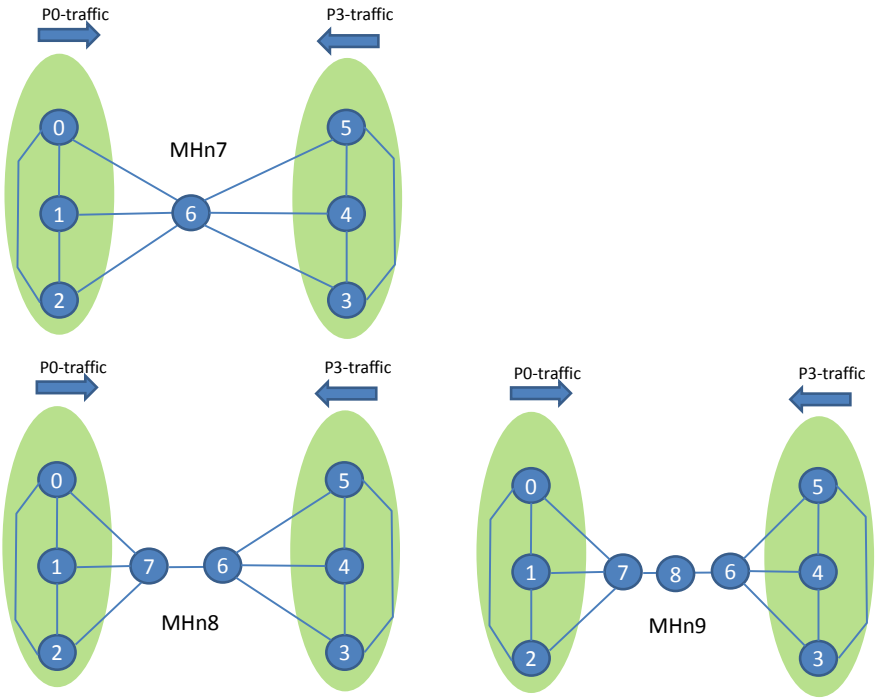

Figure 7.1 Three multihop scenarios MHn7, MHn8 and MHn9.

[11] Statistics are also collected when a packet is deleted by the lifetime control function.

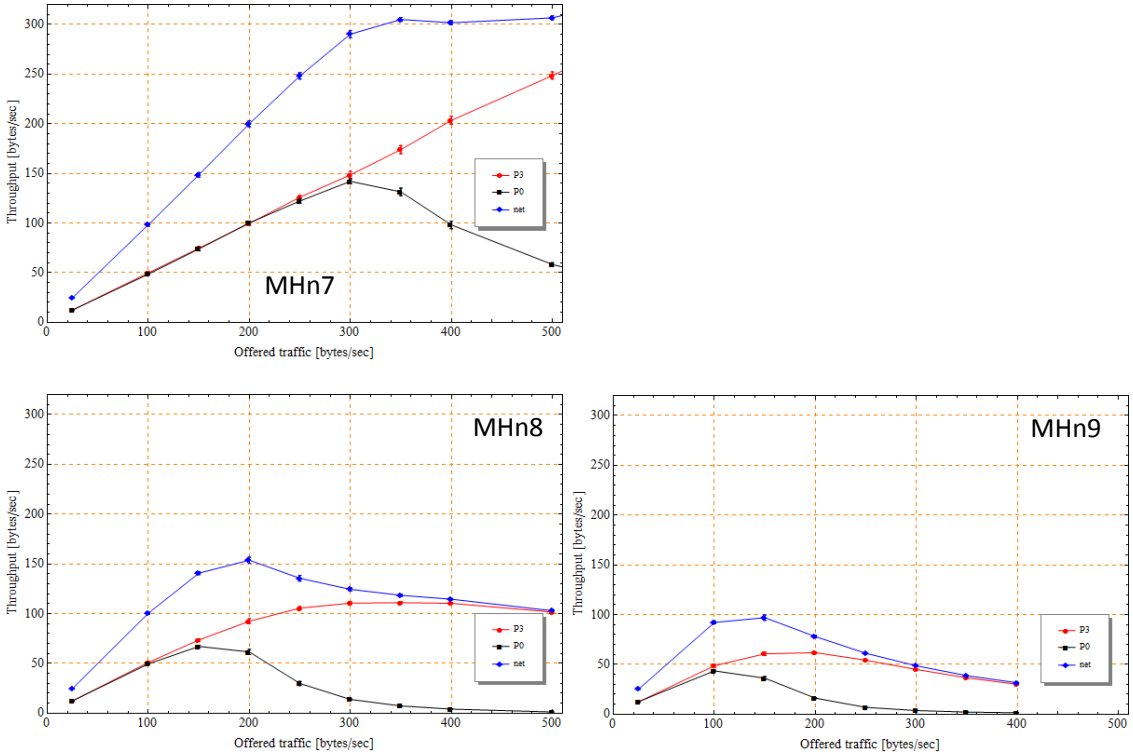

Figure 7.2 Throughput vs. offered traffic in the multihop networks (sept22/23/24).

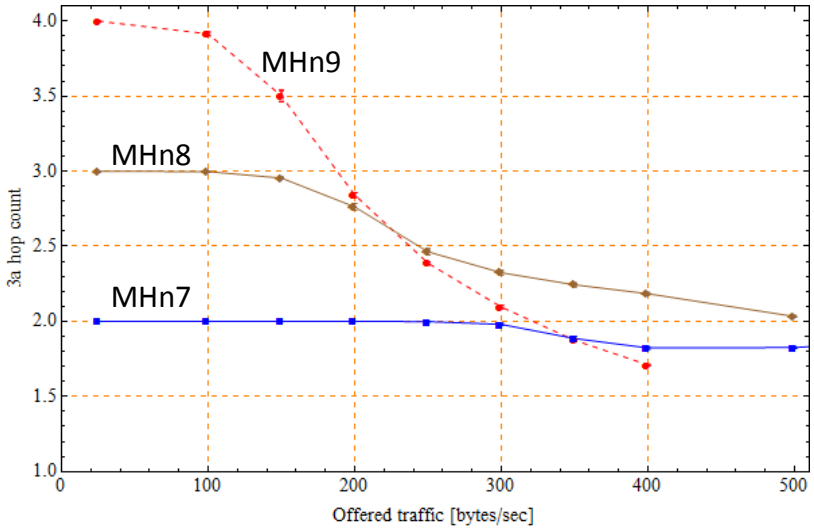

Figure 7.3 Number of radio hops vs. offered traffic.

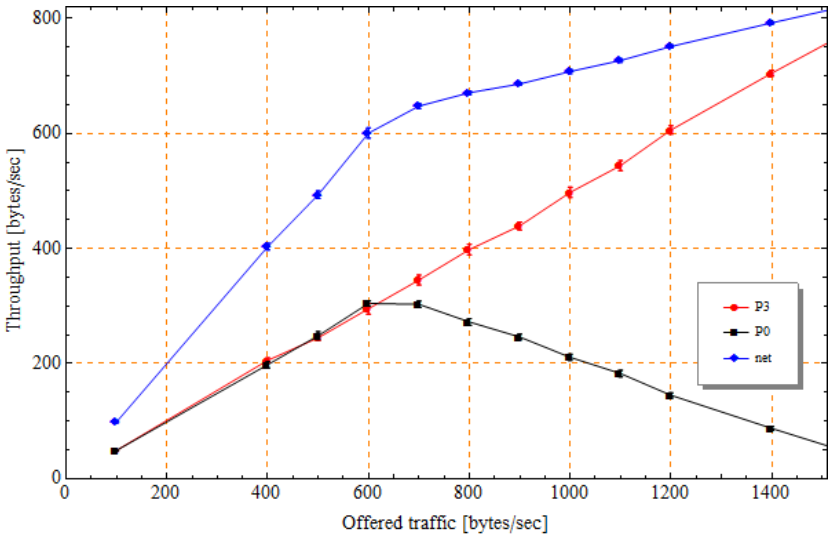

Figure 7.4 Simulated AHAn6 performance. The throughput capacity is approximately 600 bytes/s.

7.1 Protocol Efficiency

The simulation scenarios in this chapter facilitate estimation of the protocol efficiency with little additional effort. By simulating an AHAn8-network[12] using the same traffic profile as the MHn8-network and the two routing variants below, we can calculate the multihop efficiency.

C1: AHAn8 using the MHn8 routing table
C2: AHAn8 using the normal AHA-network routing table (shortest path)

C2 is the ordinary operating mode for an AHA-network where shortest path routes are used. C1 is an artificial case that estimates the cost of multihop without the presence of the hidden-nodes.

Simulation shows (Figure 7.4) that C2 has the throughput capacity 600 bytes/s. An upper limit of the throughput in the MHn8-network is 600/3 = 200 bytes/s. Figure 7.5 indicates that C1 has the throughput capacity 194±2 bytes/s, which is only 3% less than the upper limit.

[12] Only 6 nodes do generate traffic.

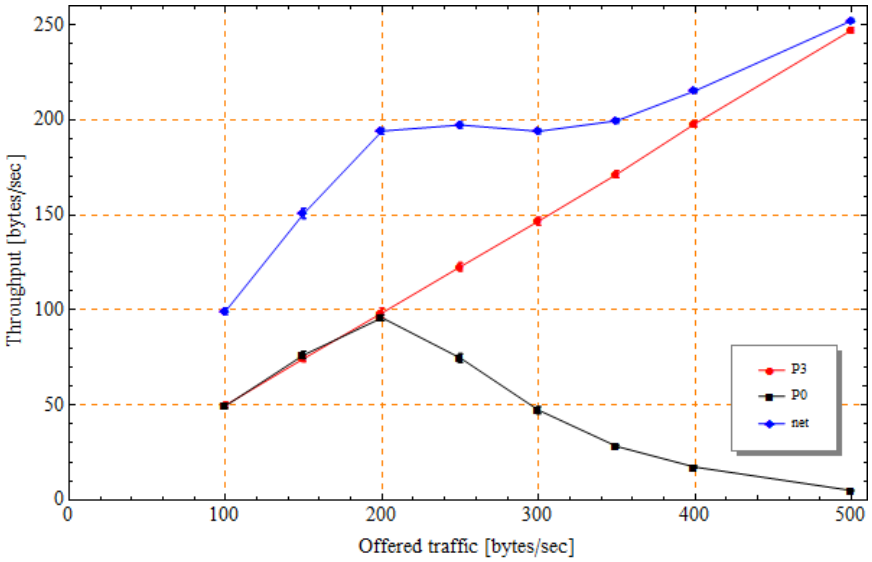

Figure 7.5 Case 1: AHAn8 using the MHn8 routing table.

7.2 Lesson Learned

In the multihop networks simulated, the NBWF protocols had an acceptable priority sorting characteristics; high priority packets were served while low priority packets were denied service (Figure 7.2). Due to the MAC CR/CC PDU signalling system, the protocol efficiency was good in the MHn7 ($\beta_{MH7} = 0.9$) network and the P3-traffic is served with significant lower end-to-end delays at all load levels, see Figure 7.6.

The traffic conditions in the MHn8 and MHn9 networks were much more demanding for the NBWF protocols and the efficiency decreases. It is very costly to lose a CC PDU; a CR PDU was received successfully and has consumed bandwidth. A possible relief of this problem is to introduce an additional MAC priority delay. Figure 7.7 illustrates how the MAC CR PDU sent by node A will synchronise the MAC scheduling process among the busy nodes in the set H_A. They cannot receive the MAC CC PDU sent by B but detect the reservation when A starts to send data. However, some of the nodes may send a CR PDU. By introducing an additional component to the priority delay as shown in Figure 7.8, the CR will be delayed sufficiently not to hit the CC. Only P3 needs this delay component (since P3 has zero priority delay), but the other levels must be delayed accordingly not to affect the priority sorting property. The delay added certainly gives some performance degradation in mesh networks and the solution should only be used in special networks.

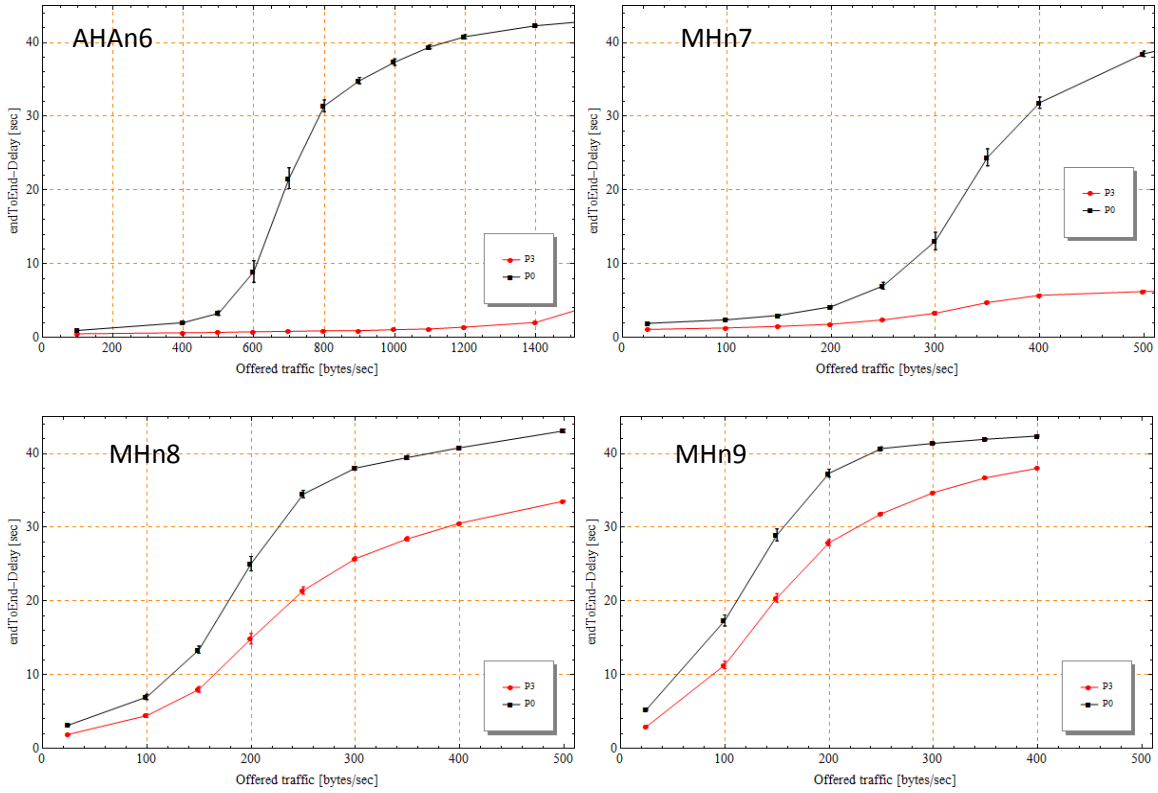

Figure 7.6 End-to-end delay vs. offered traffic.

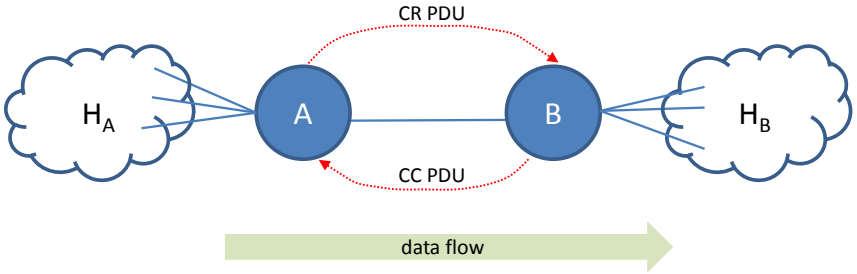

Figure 7.7 Two nodes A and B in a multihop network where the IP-flow is directed from A to B. Both nodes have hidden-nodes. Node A's hidden-node set is H_B.

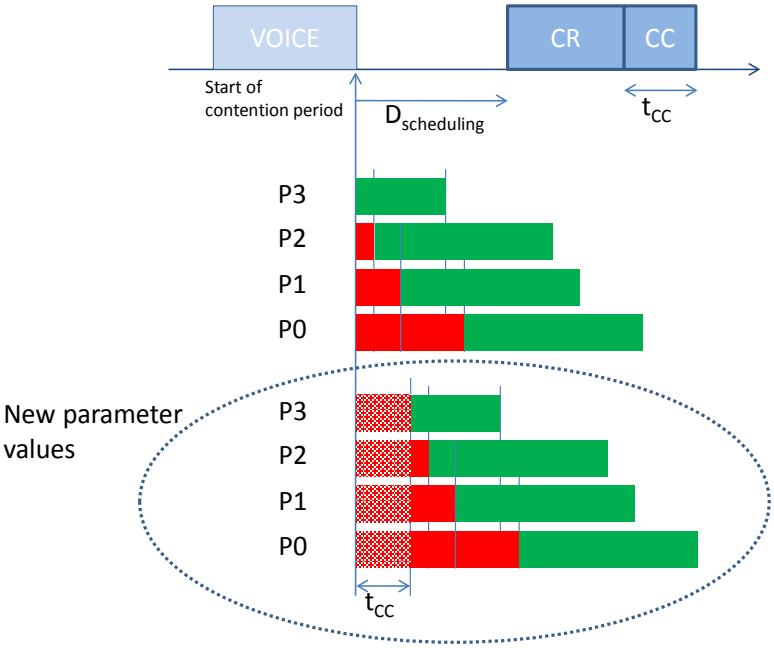

Figure 7.8 Illustration of the MAC random access delay parameter values. The red areas are priority delays while the green areas are random delays [1, chapter 5].

8 Conclusions and Remarks

Each chapter in this document ends with a "lesson learned"-section and here we give only an extract.

There exists no single MAC parameter set that can be stated as the best choice for all traffic conditions. Chapter 3 "MAC Parameter Optimization" goes through the processes of tuning the MAC parameters to a specific traffic profile and network size. The NBWF STANAGs should use the same approach to optimise the parameter values for the profiles specified in [6, chapter 8 "Profiles for the NBWF".

Possibly, the most interesting chapter is chapter 5 "GridN100 Networks" because here we gradually reduce the radio coverage in a large network and analyse how the NBWF protocols react. As the network becomes more fragmented, a number of factors contribute to degraded performance:

- The hidden-node problem increases the MAC CR PDU collision probability;
- Hidden-nodes cause MAC CC PDU losses;
- Hidden-nodes may interfere with an established MAC connection when they fail to register a successful TDMA reservation phase; and
- A part of the traffic is relayed over more than one radio hop, which consumes more transmission capacity than single-hop traffic.

Chapter 5 concludes that it is the MAC reservation protocol that gets the hardest operating condition first. But remember, the NBWF simulator does not model the routing protocol. Chapter 4 showed that the MAC reservation protocol delivers acceptable throughput in a fully meshed network with 100 nodes.

Some enhancements to the NBWF protocols are proposed. Chapter 3 proposed that the LLC-layer and the 3a-layer should discard a packet if the remaining lifetime is below a certain threshold. Chapter 7 suggested adding an additional MAC priority delay to protect the MAC CC PDU in presence of hidden-nodes. This may lead to lower throughput in other scenarios since the MAC channel idle period is increased.

References

[1] Tore J Berg, “NATO Narrowband Waveform (NBWF) – multilevel precedence and pre-emption for IP traffic”, FFI-report 2012/01884, FFI October 22st, 2012.

[2] Tore J Berg, “NATO Narrowband Waveform (NBWF)- Network Layer Flow Control Protocols”, FFI-report 2013/01899, FFI July 24th, 2013.

[3] Tore J Berg, “Design of an initial LLC Data Protocol for the NBWF Simulator”, FFI-report 2011/00537, FFI March 21st, 2012.

[4] Egli J J, “Radio propagation above 40 MC over irregular terrain”, Proceedings of the IRE, Oct 1957, pp 1383-1391.

[5] Egli model, http://en.wikipedia.org/wiki/Egli_Model.

[6] NATO STANAG 5630, “Narrowband waveform for VHF/UHF Radio – Head Stanag”, Draft edition December 2014.

[7] NATO STANAG 5631, “Narrowband waveform for VHF/UHF Radios – Physical Layer Standard and Propagation Models”, Draft edition September 2014.

[8] NATO STANAG 5632, “Narrowband waveform for VHF/UHF Radios – Link Layer Standard”, Draft edition December 2014.

[9] NATO STANAG 5633, “Narrowband waveform for VHF/UHF Radios – Network Stanag”, Draft edition November 2014.

[10] Vivianne Jodalen, et.al, “NATO Narrowband Waveform (NBWF) – overview of link layer design”, FFI-report 2009/01894, FFI March 28th, 2011.

[11] Tore J Berg, “The design of an initial NBWF network simulator”, FFI-report 2008/01921, FFI November 24th 2008.

[12] Svein Haavik, ”Initial link layer protocol design for NBWF – input to NATO SC/6 – AHWG/2”, FFI-report 2009/01895.

[13] Vivianne Jodalen, ”Modelling the NBWF radio”, TIPPER/FFI project document, FFI June 2008.

[14] Bjørnar Libæk, et.al, “Enhancements to the Narrowband Waveform (NBWF) network simulator”, FFI-report 2009/01765, FFI June 10th 2008.

[15] Bjørnar Libæk and Bjørn Solberg, “A simulator model of the NATO Narrowband Waveform physical layer”, FFI-notat 2011/00533, FFI October 19th, 2011.

Terms and Acronyms

λ_C	Throughput capacity
λ_{max}	Maximum throughput
AHA	All hearing all
ARQ	Automatic Repeat Request
CAS	Carrier sense
CC	Connect Confirm
CC PDU	Connect Confirm PDU
CL	ConnectionLess
CNR	Combat Net Radio
CO	Connection Oriented
CR	Connect Request
CR PDU	Connect Request PDU
CTS	Clear To Send
DC	Disconnect Confirm
DR-PDU	Disconnect Request PDU
DSSS	Direct Sequence Spread Spectrum
DT PDU	Data PDU
EFD	Estimated Forward Delay
EPM	Electronic Protective Measures
FSM	Finite State machine
GUID	Global Unique Identifier
H_A	Hidden node set for node A
ICI	Interface Control Information
IFD	Initial Forward Delay
IP	Internet Protocol
LLC	Logical Link Control
LLCE	LLC Entity
MAC	Medium Access Control
MACE	MAC Entity
MAC-SP	MAC Service Provider
MANET	Mobile Ad-hoc NETwork
MFD	Measured Forward Delay
MLL-report	MAC Load Level Report
MLPP	Multi-Level Precedence and Preemption
NBWF	Narrow Band Wave Form
NC3B	NATO C3 Board
NLFC	Network Level Flow Control
OSI	Open System Interconnection
PCAS	Premature CAS
p_{CC}	Probability to receive a CC PDU after sending a CR PDU
PCI	Protocol Control Information
PDP	Packet Data Protocol
PDU	Protocol Data Unit

PECN	Periodic Explicit Notification
PHY	Physical
PSMA	Preamble Sense Multiple Access
PTT	Push To Talk
QoS	Quality of Service
RF	Radio Frequency
RTS	Request To Send
SAP	Service Access Point
SDU	Service Data Unit
SNR	Signal to Noise Ratio
SOM	Start Of Message
TDM	Time Division Multiplexing
TDMA	Time Division Multiple Access